International Journal of Control

ISSN: 0020-7179 (Print) 1366-5820 (Online) Journal homepage: https://www.tandfonline.com/loi/tcon20

A numerical approach to hybrid nonlinear optimal control

Esmaeil Sharifi & Christopher J. Damaren

To cite this article: Esmaeil Sharifi & Christopher J. Damaren (2020): A numerical approach to hybrid nonlinear optimal control, International Journal of Control, DOI: 10.1080/00207179.2020.1763471

To link to this article: https://doi.org/10.1080/00207179.2020.1763471

Accepted author version posted online: 03 May 2020.
Published online: 14 May 2020.

INTERNATIONAL JOURNAL OF CONTROL
https://doi.org/10.1080/00207179.2020.1763471

Taylor & Francis
Taylor & Francis Group

A numerical approach to hybrid nonlinear optimal control

Esmaeil Sharifi and Christopher J. Damaren

Institute for Aerospace Studies, University of Toronto, Toronto, Canada

ABSTRACT

This paper proposes a novel optimal control design framework for hybrid nonlinear dynamical systems involving an interacting combination of continuous-time and discrete-time dynamics. Two numerical algorithms are proposed to approximate the continuous-time and discrete-time portions of the hybrid Hamilton-Jacobi-Bellman (HJB) equation. Galerkin's spectral method is utilised to approximate the value function involved in the continuous-time HJB equation, thereby computing the optimal control gains between impulsive events. Employing the spectral collocation method, the discrete-time HJB equation is then approximated to find the optimal control gain vector at impulsive instants. These two algorithms are ultimately combined to obtain the desired hybrid nonlinear optimal control law. Describing practical considerations for implementing the algorithms, some illustrative examples are presented to evaluate the functionality of the proposed hybrid nonlinear optimal controller.

ARTICLE HISTORY
Received 8 October 2019
Accepted 27 April 2020

KEYWORDS
Hybrid nonlinear dynamical systems; hybrid nonlinear optimal control; Hamilton-Jacobi-Bellman equation; Galerkin-based approximation; collocation-based approximation

1. Introduction

Modern complex engineering systems typically involve multiple modes of operation, placing stringent demands on controller design and implementation of increasing complexity. Such systems possess an interacting mixture of continuous-time and discrete-time dynamics, exhibiting discontinuous flows on appropriate manifolds, and hence give rise to hybrid dynamics (Haddad et al., 2006). The ability to develop a control design framework for hybrid dynamical systems is therefore crucial considering the increasingly complex nature of such systems, including advanced high-performance tactical fighter aircrafts, air transportation systems, and swarms of air and space vehicles to name but a few (Haddad et al., 2006).

Hybrid dynamical systems, as an emerging discipline within dynamical systems theory and control, can be defined as an interacting countable collection of dynamical systems involving a mixture of continuous-time dynamics and discrete-time events (Haddad et al., 2006). Such systems consist of three major elements; a continuous-time set of differential equations, which characterises the motion of the dynamical system between impulsive events, a set of difference equations, which governs the way through which the states of the system are instantaneously changed when an impulse occurs, and a criterion to determine when impulses are to be applied (i.e. when the states of the system are to be reset). For example, mechanical systems subject to unilateral constraints on system positions introduce hybrid dynamical systems. These systems involve discontinuous solutions wherein discontinuities arise primarily from impacts when the system trajectories encounter the unilateral constraints (Haddad et al., 2006). Since hybrid dynamical systems can involve impulses at variable times, they are in general time-varying systems wherein the impulsive events are both a function of time and the system's state.

Although the control theory for hybrid nonlinear dynamical systems is well-developed (See Haddad et al., 2006 and references therein), there have been no applications due to the lack of efficient numerical methods for dealing with these systems. This paper aims to bridge the gap between theory and practice by developing a novel optimal control design framework for hybrid nonlinear dynamical systems involving an interacting combination of continuous-time and discrete-time dynamics. Modern spacecraft with mass expulsion devices (thrusters) are good examples to illustrate the main motivation behind this work. Being equipped with propellantless propulsion technology as a continuous-time renewable source of actuation, such systems exchange energy and momentum with the environment wherein the spacecraft operates as well as expending propellant (solar sails (McInnes, 1999) and electrodynamic tethers (Cosmo & Lorenzini, 1997) are examples of propellantless propulsion systems which interact with the sun and a planet's magnetic field respectively for actuation). Since impulsive actuation provided by thrusters is directly related to expendable chemical fuel, an optimal set of impulsive thrusting, including optimal impulsive control inputs and the optimal time instants at which impulses are to be applied, is thus required to reduce fuel usage, thereby extending the duration of such space missions. Furthermore, by optimal combination of continuous-time control input and impulsive thrusts, the use of both continuous-time and impulsive control inputs is optimised, hence the hybrid performance index is significantly improved.

The proposed hybrid algorithm has a wide range of applications amongst which two practical space applications, namely magnetic/impulsive spacecraft attitude control (Sharifi & Damaren, 2020b) and Lorentz/impulsive spacecraft formation flying (Sharifi & Damaren, 2019), will be the subject of forthcoming papers of the current authors. In both cases, a

CONTACT Esmaeil Sharifi esmaeil.sharifi@mail.utoronto.ca Institute for Aerospace Studies, University of Toronto, Toronto, Canada

continuous-time controller actuated by the Earth's magnetic field, as a renewable source of actuation, is optimally combined with impulsive thrusts to resolve the uncontrollability issues inherently involved in the continuous-time subsystem, and accordingly correct the orientation and orbital motion of the spacecraft respectively.

Simultaneous use of continuous-time and impulsive control inputs was studied by Sobiesiak and Damaren (2015a) wherein the so-called hybrid linear quadratic regulator (LQR) policy was proposed with a prescribed set of impulses to combine the two modes of actuation, namely Lorentz force and impulsive thrusting, in an optimal manner for spacecraft formation flying. Deriving the necessary and sufficient conditions for minimising a performance index with respect to impulse times, optimal thrust application times for an impulsive formation keeping and reconfiguration strategy was determined in (Sobiesiak & Damaren, 2015b). The hybrid LQR theory proposed in (Sobiesiak & Damaren, 2015a) was then extended such that the performance index was minimised with respect to continuous-time and impulsive control inputs as well as impulsive application times (Sobiesiak & Damaren, 2016).

The objective of this paper is to extend the solution of hybrid optimal control problems to nonlinear systems. Using the control scheme proposed in this research work, feedback controllers are synthesised by considering the full nonlinear dynamics of the system. No linearisation is involved, neither dynamic feedback linearisation nor a priori linearisation of the equations of motion. This is particularly useful for systems wherein the required range of operation is large (hence linear approximation is invalid) and nonlinear controllers are therefore required to appropriately compensate for the nonlinearities involved in the system. For such systems, a nonlinear control law defined over the entire operating range of the system would reduce the complexity and cost of the system while simultaneously increasing the functional performance.

Two design algorithms are proposed in this paper to approximate the hybrid version of the Hamilton-Jacobi-Bellman (HJB) equation, thereby addressing the hybrid nonlinear optimal control problem being considered. Galerkin's spectral method (Fletcher, 1984) is used to approximate the value function involved in the continuous-time HJB equation, thereby computing the continuous-time optimal control law. Employing the spectral collocation method (Quarteroni et al., 2000), the discrete-time HJB equation is subsequently approximated to derive the discrete-time counterpart of the hybrid algorithm. In the following, the historical background and the main idea behind each approach are briefly described.

Motivated by the success of optimal control methods for linear systems like the LQR technique, there has been a great deal of research devoted to extending this concept to nonlinear systems. From optimal control theory, it is well-known that when the system is modelled by nonlinear dynamics or the cost functional to be optimised is non-quadratic, the optimal control is then a state feedback function that depends upon the solution to the HJB equation (Lewis et al., 2012). Since the HJB equation is extremely difficult to solve in general, approximation techniques are thus necessitated. If an open-loop solution is acceptable, there are several methods to solve the optimal control problem. A common approach is to numerically solve for the state and co-state equations obtained from a Hamiltonian formulation of the optimal control problem. The problem can be then reduced to a two-point boundary value problem which can be solved by various methods (Beard, 1995).

Since open-loop control is undesirable for practical systems, various approaches have been investigated to generate closed-loop solutions to the HJB equation. One technique is the perturbation method wherein the nonlinear system is assumed to be a perturbation of a linear system. The approximation is then formed by finding a finite number of terms involved in a Taylor series expansion of the value function (Garrard & Jordan, 1977; Nishikawa et al., 1971). Perturbation methods are, however, limited to systems with analytic optimal cost and control which only deviate slightly from a linear system. Another approach is to regularise the cost function so that an analytic expression for the control can be obtained. The basic idea is to consider a cost function consisting of a term chosen such that the HJB equation reduces to a form similar to the Riccati equation (Freeman & Kokotovic, 1995; Lu, 1993). Although this approach results in solutions that stabilise the system, it is difficult to estimate how far the control deviates from the optimal solution. Feedback linearisation is another technique which uses feedback to cancel out the nonlinearities involved in the system (Isidori, 1989; Nijmeijer & van der Schaft, 1990). The drawback associated with feedback linearisation is that the control sometimes cancels out nonlinearities that enhance the stability and performance of the system. Moreover, the control effort used to cancel the nonlinearities can be unreasonably large. Neural networks can be also trained by computing open-loop controls for various points in the state space to approximate the solution of the HJB equation (Abu-Khalaf & Lewis, 2005; Cheng et al., 2007; Liu et al., 2009). Nevertheless, there is no guarantee for the stability of the closed-loop system via this approach. Furthermore, finite difference and finite element techniques have been used to approximate the HJB equation (Bardi & Capuzzo-Dolcetta, 2008; Richardson & Wang, 2006; Wang et al., 2003). These methods, however, suffer from the curse of dimensionality since the computational load and computer memory required for the approximation grow exponentially with the dimension of the state of the system. A survey of research directed toward approximating the HJB equation can be found in (Beard, 1995) and (Beard & McLain, 1998b).

Galerkin's spectral method can be used to find a uniform approximation to the continuous-time HJB equation such that the approximate controls are still stable on a specified set (Beard, 1995). The successive Galerkin approximation (SGA), which simultaneously combines successive approximation and Galerkin approximation, introduces a design algorithm which systematically improves the closed-loop performance of arbitrary stabilising feedback control laws (Beard, 1995). The basic idea behind successive approximation is to compute the value function involved in the HJB equation and the associated optimal control iteratively, instead of calculating them simultaneously (Beard, 1995; Beard & McLain, 1998b). The essence of the SGA approach is first to reduce the continuous-time HJB equation, which is a nonlinear partial differential equation, to a sequence of linear first-order partial differential equations known as the Generalized Hamilton-Jacobi-Bellman (GHJB) equation. Galerkin's approximation method is then utilised

with basis functions defined globally on a compact set to approximate these partial differential equations (Beard, 1995). Starting with an arbitrary stabilising control law, the GHJB equation is first solved for the value function associated with this initial control law, and the optimal control in terms of the value function is then updated. When this process is iterated, the solution to the GHJB equation converges uniformly to the solution of the continuous-time HJB equation, which consequently solves the optimal control problem being considered (Beard, 1995).

The SGA algorithm to approximate the continuous-time HJB equation first appeared in (Beard, 1995) and then in (Beard et al., 1996) along with some illustrative examples for time-invariant control systems. While the convergence of Galerkin's approximation for the GHJB equation was shown in (Beard et al., 1997), the convergence of the SGA algorithm for the continuous-time HJB equation was demonstrated in (Beard et al., 1998a). In (Beard & McLain, 1998b) and (Lawton & Beard, 1998), the authors showed how the structure of the algorithm can be exploited to reduce the amount of computations from exponential to polynomial growth in the dimension of the state space. The SGA algorithm was then applied to some real-world problems; including a hydraulically actuated positioning system (McLain & Beard, 1997), an underwater robotic vehicle (McLain & Beard, 1998a), a missile autopilot (McLain & Beard, 1998b), and an attitude control problem (Lawton et al., 1999); to design nonlinear optimal control for the infinite-time horizon systems being considered.

Inspired by (Beard, 1995), the continuous-time HJB equation is approximated by the direct application of the Galerkin method in this paper to synthesise the nonlinear optimal control for finite-time horizon systems. Using successive approximation to solve the GHJB equation in a finite-time horizon setting has the advantage of producing a linear set of differential equations to be solved for the unknown time-dependent coefficients; hence no escape in finite-time occurs (Beard, 1995). However, it is difficult to find a well-defined stabilising control law to initialise the algorithm with; especially when the time interval is small, hence asymptotic convergence is difficult or even impossible. Therefore, the differential equations through which the time-varying control gains are to be computed may become severely ill-conditioned. As opposed to this, the algorithm proposed in this paper, which applies Galerkin's spectral method directly to the continuous-time HJB equation, is completely independent of any initial stabilising control law. However, the corresponding differential equations to be solved for the time-varying control gains are nonlinear, hence finite-time escape is possible.

As mentioned at the outset, impulsive events are one of the three elements of hybrid dynamical systems. They introduce discontinuities in the states of a hybrid dynamical system once a specific criterion, which determines when the states of the system are to be reset, is met. Utilising an optimal control policy to address impulsive control problems, a variational method was proposed in (Bryson & Ho, 1975) for systems whose states experience discontinuities at interior points. In addition, the impulsive maximum principle (Blaquière, 1977) was applied to the linear quadratic control problem of switched continuous-time systems with impulsive inputs by Hu et al. (2005). This work was then extended by (Sobiesiak & Damaren, 2015a) to explicitly show how the solution to the Riccati equation resets when the discrete-time dynamics are applied. The current paper proposes a novel algorithm to derive the discrete-time portion of a hybrid nonlinear optimal control law. The proposed approach uses the spectral collocation method to approximate the discrete-time HJB equation, hence compute the optimal control gain vector at impulsive instants. The main idea behind the collocation method is to project the discrete-time HJB equation onto a discrete basis to produce as many equations as required for the unknowns. This is analogous to Galerkin's spectral method wherein the error function resulting from approximating the value function is projected onto a set of basis elements to obtain N simultaneous equations in N unknows.

This paper is organised as follows. Defining a hybrid nonlinear optimal control problem involving a hybrid performance index in section 2, hybrid versions of Bellman's principle of optimality and the HJB equation are first presented. The hybrid performance functional being considered is then related to an underlying Lyapunov function in a specific way. This Lyapunov function is subsequently shown to solve the hybrid HJB equation, thereby guaranteeing the optimality and asymptotic stability of the hybrid control system. Two separate numerical schemes are then proposed in subsections 2.1 and 2.2 to approximate the continuous-time and discrete-time portions of the hybrid HJB equation respectively. Combining these two algorithms, the desired hybrid nonlinear optimal control law is ultimately presented in subsection 2.3. Section 3 describes practical considerations for implementing the proposed hybrid algorithm. Two illustrative examples are lastly presented in section 4 to evaluate the functionality of the proposed hybrid controller.

2. Hybrid nonlinear optimal control

In this section, a hybrid feedback nonlinear optimal control problem is considered over a finite-time horizon, assuming a hybrid non-quadratic performance index. This hybrid performance functional involves two portions: a continuous-time cost, which addresses the performance of the continuous-time dynamics between impulsive events, and a discrete-time cost, which evaluates the performance of the discrete-time dynamics when impulses are applied. Consider a hybrid system modelled by nonlinear equations of the form (Haddad et al., 2001)

$$\begin{cases} \dot{\boldsymbol{x}}(t) = \boldsymbol{F}_{ct}(\boldsymbol{x}(t), \boldsymbol{u}_{ct}(t), t),\ \boldsymbol{x}(t_0) = \boldsymbol{x}_0, \\ \qquad\qquad \boldsymbol{u}_{ct} \in \boldsymbol{U}_{ct}\ (\boldsymbol{x}, t) \notin \mathcal{S} \\ \Delta\boldsymbol{x}(t)\ = \boldsymbol{x}(t^+) - \boldsymbol{x}(t) = \boldsymbol{F}_{ds}(\boldsymbol{x}(t), \boldsymbol{u}_{ds}(t), t), \\ \qquad\qquad \boldsymbol{u}_{ds} \in \boldsymbol{U}_{ds}\ (\boldsymbol{x}, t) \in \mathcal{S} \end{cases} \tag{1}$$

where $t \geq 0, \boldsymbol{x} \in \mathcal{D} \subseteq \mathbb{R}^n$ is the state vector, $\mathcal{D}$ specifies an open set with $\mathbf{0} \in \mathcal{D}$, $(\boldsymbol{u}_{ct}, \boldsymbol{u}_{ds}) \in \boldsymbol{U}_{ct} \times \boldsymbol{U}_{ds} \subseteq \mathbb{R}^{m_{ct}} \times \mathbb{R}^{m_{ds}}$ denotes the hybrid control input, $\boldsymbol{F}_{ct} : \mathcal{D} \times \boldsymbol{U}_{ct} \times \mathbb{R} \to \mathbb{R}^n$ is Lipschitz continuous satisfying $\boldsymbol{F}_{ct}(\mathbf{0}, \mathbf{0}, t) = \mathbf{0}$ for every $t \in [t_0, t_f]$, $\boldsymbol{F}_{ds} : \mathcal{S} \times \boldsymbol{U}_{ds} \to \mathbb{R}^n$ is continuous and satisfies $\boldsymbol{F}_{ds}(\mathbf{0}, \mathbf{0}, t) = \mathbf{0}$ for every $t \in [t_0, t_f]$, and $\mathcal{S} \subset \mathbb{R}^n \times [0, \infty)$ denotes the resetting set. It is also assumed that $(\boldsymbol{u}_{ct}, \boldsymbol{u}_{ds})$ is restricted to the class

of admissible control inputs $\mathcal{U}_{ct} \times \mathcal{U}_{ds}$ consisting of measurable functions such that $(\boldsymbol{u}_{ct}, \boldsymbol{u}_{ds}) \in \boldsymbol{U}_{ct} \times \boldsymbol{U}_{ds}$, where the constraint set $\boldsymbol{U}_{ct} \times \boldsymbol{U}_{ds}$ is given with $(\boldsymbol{0}, \boldsymbol{0}) \in \boldsymbol{U}_{ct} \times \boldsymbol{U}_{ds}$. The main objective is then to determine a hybrid nonlinear control input $(\boldsymbol{u}_{ct}, \boldsymbol{u}_{ds}) \in \boldsymbol{U}_{ct} \times \boldsymbol{U}_{ds}$ such that the following hybrid performance index is minimised over all admissible control inputs $(\boldsymbol{u}_{ct}, \boldsymbol{u}_{ds}) \in \mathcal{U}_{ct} \times \mathcal{U}_{ds}$ (Haddad et al., 2001):

$$J(\boldsymbol{x}_0, \boldsymbol{u}_{ct}, \boldsymbol{u}_{ds}, t_0) = \int_{t_0}^{t_f} L_{ct}(\boldsymbol{x}(t), \boldsymbol{u}_{ct}(t), t)dt + \sum_{k=1}^{N_{imp}} L_{ds}(\boldsymbol{x}(t_k), \boldsymbol{u}_{ds}(t_k), t_k) \tag{2}$$

where $L_{ct} : \mathcal{D} \times \boldsymbol{U}_{ct} \times \mathbb{R} \to \mathbb{R}$ and $L_{ds} : \mathcal{S} \times \boldsymbol{U}_{ds} \to \mathbb{R}$ are, respectively, the continuous-time and discrete-time instantaneous cost functions, t_k specifies the time instants at which impulses are to be applied with $k \in \mathbb{Z}_{(t_0,t_f)}$, and N_{imp} is the number of impulses during the operating time.

Given a hybrid control input $(\boldsymbol{u}_{ct}, \boldsymbol{u}_{ds}) \in \boldsymbol{U}_{ct} \times \boldsymbol{U}_{ds}$, the necessary and sufficient conditions for minimising the hybrid performance index (2) are then obtained via a hybrid version of Bellman's principle of optimality as below (Haddad et al., 2001).

Lemma 2.1: *Let $(\boldsymbol{u}^*_{ct}, \boldsymbol{u}^*_{ds}) \in \mathcal{U}_{ct} \times \mathcal{U}_{ds}$ be a hybrid optimal control that generates the trajectory $\boldsymbol{x}(t)$, $t \in [t_0, t_f]$, with $\boldsymbol{x}(t_0) = \boldsymbol{x}_0$. Then the trajectory $\boldsymbol{x}$ from $(\boldsymbol{x}_0, t_0)$ to $(\boldsymbol{x}_f, t_f)$ is optimal if and only if for all $t', t'' \in [t_0, t_f]$, the portion of the trajectory $\boldsymbol{x}$ going from $(\boldsymbol{x}(t'), t')$ to $(\boldsymbol{x}(t''), t'')$ optimises the same cost functional over $[t', t'']$, where $\boldsymbol{x}_f \triangleq \boldsymbol{x}(t_f)$ and $\boldsymbol{x}(t')$ is a point on the optimal trajectory generated by $(\boldsymbol{u}^*_{ct}, \boldsymbol{u}^*_{ds})$.*

***Proof**: Refer to (Haddad et al., 2001) or (Haddad et al., 2006, Chapter 9).*

In addition, by relating the hybrid performance index (2) to an underlying Lyapunov function in a judicious way, the asymptotic stability of the hybrid nonlinear closed-loop system is consequently guaranteed. This Lyapunov function is shown to be a solution of the hybrid HJB equation via the following theorems, thereby guaranteeing both optimality and asymptotic stability of the hybrid feedback control system (Haddad et al., 2001).

Let $(\boldsymbol{u}^*_{ct}, \boldsymbol{u}^*_{ds})$ solve the hybrid optimal control problem (1), and define the optimal cost $J^*(\boldsymbol{x}_0, t_0) \triangleq J(\boldsymbol{x}_0, \boldsymbol{u}^*_{ct}, \boldsymbol{u}^*_{ds}, t_0)$. Furthermore, define the Hamiltonians associated with the continuous-time and discrete-time dynamics for $\boldsymbol{p} \in \mathbb{R}^n$ and $q : \mathbb{R}^n \times \mathbb{R} \to \mathbb{R}$ as follows:

$$\mathcal{H}_{ct}(\boldsymbol{x}, \boldsymbol{u}_{ct}, \boldsymbol{p}(\boldsymbol{x}, t), t) \triangleq L_{ct}(\boldsymbol{x}, \boldsymbol{u}_{ct}, t) + \boldsymbol{p}^{\mathrm{T}}(\boldsymbol{x}, t) \times \boldsymbol{F}_{ct}(\boldsymbol{x}, \boldsymbol{u}_{ct}, t) \tag{3}$$

$$\mathcal{H}_{ds}(\boldsymbol{x}, \boldsymbol{u}_{ds}, q(\boldsymbol{x}, t_k), t_k) \triangleq L_{ds}(\boldsymbol{x}, \boldsymbol{u}_{ds}, t_k) + q(\boldsymbol{x} + \boldsymbol{F}_{ds}(\boldsymbol{x}, \boldsymbol{u}_{ds}, t_k), t_k) - q(\boldsymbol{x}, t_k) \tag{4}$$

Theorem 2.2: *Let $J^*(\boldsymbol{x}, t)$ denote the minimal cost for the hybrid optimal control problem (1) with $\boldsymbol{x}_0 = \boldsymbol{x}$ and $t_0 = t$, and assume that J^* is continuously differentiable in $\boldsymbol{x}$. Then:*

$$\frac{\partial J^*(\boldsymbol{x},\, t)}{\partial t} + \min_{\boldsymbol{u}_{ct} \in \mathcal{U}_{ct}} \{\mathcal{H}_{ct}(\boldsymbol{x}, \boldsymbol{u}_{ct}, \boldsymbol{p}(\boldsymbol{x}, t), t)\} = 0 \qquad (\boldsymbol{x}, t) \notin \mathcal{S} \tag{5}$$

$$\min_{\boldsymbol{u}_{ds} \in \mathcal{U}_{ds}} \{\mathcal{H}_{ds}(\boldsymbol{x}, \boldsymbol{u}_{ds}, q(\boldsymbol{x}, t_k), t_k)\} = 0 \qquad (\boldsymbol{x}, t) \in \mathcal{S} \tag{6}$$

where $\boldsymbol{p}(\boldsymbol{x}, t) \triangleq \frac{\partial J^*(\boldsymbol{x},t)}{\partial \boldsymbol{x}}$ and $q(\boldsymbol{x}, t_k) \triangleq J^*(\boldsymbol{x}, t_k)$. Furthermore, if $(\boldsymbol{u}^*_{ct}, \boldsymbol{u}^*_{ds})$ solves the hybrid optimal control problem (1), then:

$$\frac{\partial J^*(\boldsymbol{x},\, t)}{\partial t} + \mathcal{H}_{ct}(\boldsymbol{x}, \boldsymbol{u}^*_{ct}, \boldsymbol{p}(\boldsymbol{x}, t), t) = 0 \qquad (\boldsymbol{x}, t) \notin \mathcal{S} \tag{7}$$

$$\mathcal{H}_{ds}(\boldsymbol{x}, \boldsymbol{u}^*_{ds}, q(\boldsymbol{x}, t_k), t_k) = 0 \qquad (\boldsymbol{x}, t) \in \mathcal{S} \tag{8}$$

***Proof**: Refer to (Haddad et al., 2001) or (Haddad et al., 2006, Chapter 9).*

Next, a converse result to Theorem 2.2 is obtained as below (Haddad et al., 2001).

Theorem 2.3: *Suppose there exists a continuously differentiable function $V : \mathcal{D} \times \mathbb{R} \to \mathbb{R}$ and a hybrid optimal control $(\boldsymbol{u}^*_{ct}, \boldsymbol{u}^*_{ds})$ such that $V(\boldsymbol{x}_f,\, t_f) = 0$ and*

$$\frac{\partial V(\boldsymbol{x},\, t)}{\partial t} + \mathcal{H}_{ct}\left(\boldsymbol{x}, \boldsymbol{u}^*_{ct}, \frac{\partial V(\boldsymbol{x}, t)}{\partial \boldsymbol{x}}, t\right) = 0 \qquad (\boldsymbol{x}, t) \notin \mathcal{S} \tag{9}$$

$$\mathcal{H}_{ds}(\boldsymbol{x}, \boldsymbol{u}^*_{ds}, V(\boldsymbol{x}, t_k), t_k) = 0 \qquad (\boldsymbol{x}, t) \in \mathcal{S} \tag{10}$$

$$\mathcal{H}_{ct}\left(\boldsymbol{x}, \boldsymbol{u}^*_{ct}, \frac{\partial V(\boldsymbol{x}, t)}{\partial \boldsymbol{x}}, t\right) \leq \mathcal{H}_{ct}\left(\boldsymbol{x}, \boldsymbol{u}_{ct}, \frac{\partial V(\boldsymbol{x}, t)}{\partial \boldsymbol{x}}, t\right), \quad \boldsymbol{u}_{ct} \in \mathcal{U}_{ct} \quad (\boldsymbol{x}, t) \notin \mathcal{S} \tag{11}$$

$$\mathcal{H}_{ds}(\boldsymbol{x}, \boldsymbol{u}^*_{ds}, V(\boldsymbol{x}, t_k), t_k) \leq \mathcal{H}_{ds}(\boldsymbol{x}, \boldsymbol{u}_{ds}, V(\boldsymbol{x}, t_k), t_k), \quad \boldsymbol{u}_{ds} \in \mathcal{U}_{ds} \quad (\boldsymbol{x}, t) \in \mathcal{S} \tag{12}$$

Therefore, $(\boldsymbol{u}^*_{ct}, \boldsymbol{u}^*_{ds})$ solves the hybrid optimal control problem (1), that is,

$$J^*(\boldsymbol{x}_0, t_0) = J(\boldsymbol{x}_0, \boldsymbol{u}^*_{ct}, \boldsymbol{u}^*_{ds}, t_0) \leq J(\boldsymbol{x}_0, \boldsymbol{u}_{ct}, \boldsymbol{u}_{ds}, t_0), \quad (\boldsymbol{u}_{ct}, \boldsymbol{u}_{ds}) \in \mathcal{U}_{ct} \times \mathcal{U}_{ds} \tag{13}$$

and

$$J^*(\boldsymbol{x}_0, t_0) = V(\boldsymbol{x}_0, t_0) \tag{14}$$

***Proof**: Refer to (Haddad et al., 2001) or (Haddad et al., 2006, Chapter 9).*

Now, the main theorem for characterising the hybrid feedback controllers that guarantee the closed-loop stability and simultaneously minimise a hybrid non-quadratic performance index is presented as follows (Haddad et al., 2001).

Theorem 2.4: *Consider the hybrid nonlinear system (1) with the hybrid performance functional (2). Assume there exist a continuously differentiable positive-definite function $V : \mathcal{D} \times \mathbb{R} \to \mathbb{R}$*

and a hybrid optimal control law $(\boldsymbol{u}_{ct}^*, \boldsymbol{u}_{ds}^*)$ *such that the conditions (9)-(12) are satisfied, and*

$$\dot{V}(\boldsymbol{x}, t) = \frac{\partial V(\boldsymbol{x}, t)}{\partial t} + \left(\frac{\partial V(\boldsymbol{x}, t)}{\partial \boldsymbol{x}}\right)^T \boldsymbol{F}_{ct}(\boldsymbol{x}, \boldsymbol{u}_{ct}^*, t) < 0, \quad \boldsymbol{x} \neq \boldsymbol{0} \quad (\boldsymbol{x}, t) \notin \mathcal{S} \tag{15}$$

$$\Delta V(\boldsymbol{x}, t) = V(\boldsymbol{x} + \boldsymbol{F}_{ds}(\boldsymbol{x}, \boldsymbol{u}_{ds}^*, t), t^+) - V(\boldsymbol{x}, t) \leq 0 \quad (\boldsymbol{x}, t) \in \mathcal{S} \tag{16}$$

Then, with the hybrid feedback control $(\boldsymbol{u}_{ct}^*, \boldsymbol{u}_{ds}^*)$*, there exists a neighbourhood of the origin* $\mathcal{D}_0 \subseteq \mathcal{D}$ *such that if* $\boldsymbol{x}_0 \in \mathcal{D}_0$*, the zero solution* $\boldsymbol{x}(t) \equiv \boldsymbol{0}$ *of the closed-loop system (1) is locally asymptotically stable. Furthermore,*

$$J^*(\boldsymbol{x}_0, t_0) = J(\boldsymbol{x}_0, \boldsymbol{u}_{ct}^*, \boldsymbol{u}_{ds}^*, t_0) = V(\boldsymbol{x}_0, t_0) \ , \ \boldsymbol{x}_0 \in \mathcal{D}_0 \tag{17}$$

In addition, if $\boldsymbol{x}_0 \in \mathcal{D}_0$*, then the hybrid feedback control* $(\boldsymbol{u}_{ct}^*, \boldsymbol{u}_{ds}^*)$ *minimises* $J(\boldsymbol{x}_0, \boldsymbol{u}_{ct}, \boldsymbol{u}_{ds}, t_0)$ *in the sense that*

$$J(\boldsymbol{x}_0, \boldsymbol{u}_{ct}^*, \boldsymbol{u}_{ds}^*, t_0) = \min_{(\boldsymbol{u}_{ct}, \boldsymbol{u}_{ds}) \in \mathcal{U}_{ct} \times \mathcal{U}_{ds}} \{J(\boldsymbol{x}_0, \boldsymbol{u}_{ct}, \boldsymbol{u}_{ds}, t_0)\} \tag{18}$$

Finally, if $\mathcal{D} = \mathbb{R}^n$*,* $\boldsymbol{U}_{ct} = \mathbb{R}^{m_{ct}}$*,* $\boldsymbol{U}_{ds} = \mathbb{R}^{m_{ds}}$*, and* $V(\boldsymbol{x}, t) \to \infty$ *as* $||\boldsymbol{x}|| \to \infty$*, then the zero solution* $\boldsymbol{x}(t) \equiv \boldsymbol{0}$ *of the closed-loop system (1) is globally asymptotically stable.*

Proof*: Local and global asymptotic stability is a direct consequence of (15) and (16) by applying Theorem 2.6 in (Haddad et al., 2006) to the closed-loop system (1). Conditions (17) and (18) are a direct consequence of Theorem 2.3.*

Therefore, the hybrid feedback controller, $(\boldsymbol{u}_{ct}^*, \boldsymbol{u}_{ds}^*)$, guarantees both closed-loop stability and optimality of the feedback-controlled hybrid system via the Lyapunov function.

Assuming that the resetting set $\mathcal{S}$ is defined by a prescribed sequence of impulsive times which are independent of the state $\boldsymbol{x}$, i.e. $\mathcal{S} = \mathcal{D} \times \mathcal{T} = \mathcal{D} \times \{t_1, \ldots, t_{N_{imp}}\}$, the results presented above are specialised in the following subsections to address an optimal control problem for a hybrid nonlinear system of the form

$$\dot{\boldsymbol{x}} = \boldsymbol{f}(\boldsymbol{x}, t) + \boldsymbol{g}(\boldsymbol{x}, t)\boldsymbol{u}_{ct}(\boldsymbol{x}, t), \boldsymbol{x}(\boldsymbol{0}) = \boldsymbol{x}_0 \quad t \neq t_k \tag{19}$$

$$\Delta \boldsymbol{x}(t_k) = \boldsymbol{x}(t_k^+) - \boldsymbol{x}(t_k^-) = \boldsymbol{B}_{ds}\boldsymbol{u}_{ds,k} \quad t = t_k \tag{20}$$

where $\boldsymbol{f} : \mathcal{D} \times \mathbb{R} \to \mathbb{R}^n$ and $\boldsymbol{g} : \mathcal{D} \times \mathbb{R} \to \mathbb{R}^{n \times m_{ct}}$ are assumed to be Lipschitz continuous on $\mathcal{D}$, and $\boldsymbol{u}_{ct}$ denotes the continuous-time control input. In addition, $\boldsymbol{x}(t_k^-) \in \mathcal{D}$ and $\boldsymbol{x}(t_k^+) \in \mathcal{D}$ are, respectively, the state vector immediately before and after the discrete-time dynamics are applied at $t = t_k$, $\boldsymbol{B}_{ds} \in \mathbb{R}^{n \times m_{ds}}$ is the discrete-time control input matrix, and $\boldsymbol{u}_{ds}(\boldsymbol{x}(t_k), t_k) \triangleq \boldsymbol{u}_{ds,k}$ denotes the discrete-time control input.

As stressed earlier, the nonlinear optimal control depends on the solution to the HJB equation, which is generally difficult to solve, hence approximation techniques are necessitated. Two numerical approaches are therefore employed in the following subsections to approximate the continuous-time and discrete-time portions of the hybrid HJB equation.

2.1 Numerical solution to the continuous-time HJB equation

Applying the Galerkin spectral method directly to the continuous-time portion of the hybrid HJB equation, a continuous-time set of differential equations is derived in this section to compute the time-varying optimal control gains between impulsive instants. Defining $L_{ct}(\boldsymbol{x}, \boldsymbol{u}_{ct}, t) = l_{ct}(\boldsymbol{x}) + ||\boldsymbol{u}_{ct}(\boldsymbol{x}, t)||^2_{\boldsymbol{R}_{ct}}$, (5) can be written as (Lewis et al., 2012):

$$\begin{cases} \frac{\partial V(\boldsymbol{x}, t)}{\partial t} + \min_{\boldsymbol{u}_{ct} \in \mathcal{U}_{ct}} \left\{ \left(\frac{\partial V(\boldsymbol{x}, t)}{\partial \boldsymbol{x}}\right)^{\mathrm{T}} (\boldsymbol{f}(\boldsymbol{x}, t) + \boldsymbol{g}(\boldsymbol{x}, t)\boldsymbol{u}_{ct}(\boldsymbol{x}, t)) \right. \\ \left. \quad + l_{ct}(\boldsymbol{x}) + ||\boldsymbol{u}_{ct}(\boldsymbol{x}, t)||^2_{\boldsymbol{R}_{ct}} \right\} = 0 \\ V(\boldsymbol{x}_{\mathrm{f}}, t_{\mathrm{f}}) = 0 \end{cases} \tag{21}$$

where $V : \mathcal{D} \times \mathbb{R} \to \mathbb{R}$ specifies the value function (the optimum value of the performance index), $l_{ct} : \mathcal{D} \to \mathbb{R}$ is a positive-definite function called the continuous-time state penalty function, and $\boldsymbol{R}_{ct} \in \mathbb{R}^{m_{ct} \times m_{ct}}$ denotes a symmetric positive-definite matrix called the continuous-time control penalty matrix. Minimising (21) with respect to $\boldsymbol{u}_{ct}$, the continuous-time optimal control law in terms of $V(\boldsymbol{x}, t)$ is found as follows:

$$\boldsymbol{u}_{ct}^*(\boldsymbol{x}, t) = -\frac{1}{2}\boldsymbol{R}_{ct}^{-1}\boldsymbol{g}^{\mathrm{T}}(\boldsymbol{x}, t)\frac{\partial V(\boldsymbol{x}, t)}{\partial \boldsymbol{x}} \tag{22}$$

By substituting (22) into (21), the continuous-time HJB equation can be thus formulated as:

$$\begin{cases} \mathrm{HJB}_{ct}(V) = \frac{\partial V}{\partial t} + \left(\frac{\partial V}{\partial \boldsymbol{x}}\right)^{\mathrm{T}}\boldsymbol{f} - \frac{1}{4}\left(\frac{\partial V}{\partial \boldsymbol{x}}\right)^{\mathrm{T}}\boldsymbol{g}\boldsymbol{R}_{ct}^{-1}\boldsymbol{g}^{\mathrm{T}}\frac{\partial V}{\partial \boldsymbol{x}} + l_{ct} = 0 \\ V(\boldsymbol{x}_{\mathrm{f}}, t_{\mathrm{f}}) = 0 \end{cases} \tag{23}$$

The continuous-time HJB equation, as a nonlinear partial differential equation, is difficult to solve in general, thereby necessitating approximation techniques. Galerkin's spectral method can be therefore exploited to approximate the solution to (23). The basic idea underlying the Galerkin approach is to assume that the solution of the continuous-time HJB equation can be expressed as an infinite sum of known basis functions (Beard, 1995). In addition, for the Galerkin method to be applicable, the problem must be placed in a suitable inner product space such that the projection is well-defined in terms of n-dimensional integrations (Beard, 1995). The approximation is thus restricted to a closed and bounded set in $\mathcal{D}$, namely a compact set Ω, which defines the bounded domain of the state space of interest. Consequently, it is first assumed that the value function can be discretized by an infinite series of prescribed state-dependent basis functions, which are continuous and defined everywhere on Ω, and unknown coefficients with time-dependency as below (Beard, 1995):

$$V(\boldsymbol{x}, t) := \sum_{j=1}^{\infty} c_j^*(t)\,\phi_j(\boldsymbol{x}) \tag{24}$$

From a practical perspective, using an infinite number of terms in the discretization is impossible; the approximation for $V(\boldsymbol{x}, t)$ is therefore carried one step further by considering a

truncated version of the infinite series (i.e. the first N terms) (Beard, 1995):

$$V_N(\boldsymbol{x}\,,\,t) := \sum_{j=1}^{N} c_j^*(t)\,\phi_j(\boldsymbol{x}) = \boldsymbol{\Phi}_N^{\mathrm{T}}(\boldsymbol{x})\boldsymbol{C}_N^*(t) \tag{25}$$

wherein $\boldsymbol{\Phi}_N(\boldsymbol{x}) = [\phi_1\,,\,\ldots\,,\,\phi_N]^{\mathrm{T}}$, $\boldsymbol{C}_N^*(t) = [c_1^*\,,\,\ldots\,,\,c_N^*]^{\mathrm{T}}$, and N denotes the number of basis elements, i.e. the order of approximation. Substituting (25) into (23) results in an error function due primarily to approximating the value function with $V_N(\boldsymbol{x}\,,\,t)$:

$$error(\boldsymbol{x}\,,\,t) = \mathrm{HJB}_{ct}\left(\sum_{j=1}^{N} c_j^*(t)\,\phi_j(\boldsymbol{x})\right) \tag{26}$$

Following the Galerkin method, the unknown coefficients, $\boldsymbol{C}_N^*(t)$, are determined such that the resulting error is minimised. To this end, the error is projected onto the same basis functions retained in the truncated series (the linear finite basis spanned by $\{\phi_j\}_1^N$), and the outcome is set equal to zero in order to obtain N simultaneous equations with N unknows (Beard, 1995):

$$\begin{cases} \left\langle \mathrm{HJB}_{ct}\left(\sum_{j=1}^{N} c_j^*(t)\,\phi_j(\boldsymbol{x})\right)\,,\,\boldsymbol{\Phi}_N(\boldsymbol{x})\right\rangle_{\Omega} = \boldsymbol{0} \\ \left\langle \sum_{j=1}^{N} c_j^*(t_{\mathrm{f}})\,\phi_j(\boldsymbol{x}_{\mathrm{f}})\,,\,\boldsymbol{\Phi}_N(\boldsymbol{x})\right\rangle_{\Omega} = \boldsymbol{0} \end{cases} \tag{27}$$

wherein the projection operator is the inner product in an appropriate Hilbert space defined by $\langle(\cdot)\,,\,\phi_i(\boldsymbol{x})\rangle_{\Omega} \triangleq \int_{\Omega}(\cdot)\phi_i(\boldsymbol{x})d\boldsymbol{x}$. The equation (27) represents the Galerkin-based projection of the continuous-time HJB equation in a compact form, which can be expanded as below:

$$\begin{cases} \langle\boldsymbol{\Phi}_N,\boldsymbol{\Phi}_N\rangle_{\Omega}\dot{\boldsymbol{C}}_N^*(t) + \langle\mathbf{J}_{\boldsymbol{x}}(\boldsymbol{\Phi}_N)\boldsymbol{f},\boldsymbol{\Phi}_N\rangle_{\Omega}\boldsymbol{C}_N^*(t) \\ \quad -\frac{1}{4}\left[\sum_{\mathrm{k}=1}^{N} c_{\mathrm{k}}^*(t)\left\langle\mathbf{J}_{\boldsymbol{x}}(\boldsymbol{\Phi}_N)\boldsymbol{g}\boldsymbol{R}_{ct}^{-1}\boldsymbol{g}^{\mathrm{T}}\frac{\partial\phi_{\mathrm{k}}}{\partial\boldsymbol{x}},\boldsymbol{\Phi}_N\right\rangle_{\Omega}\right]\boldsymbol{C}_N^*(t) \\ \quad +\langle l_{ct},\boldsymbol{\Phi}_N\rangle_{\Omega} = \boldsymbol{0} \\ \\ \langle\boldsymbol{\Phi}_N,\boldsymbol{\Phi}_N\rangle_{\Omega}\boldsymbol{C}_N^*(t_{\mathrm{f}}) = \boldsymbol{0} \end{cases} \tag{28}$$

wherein $\mathbf{J}_{\boldsymbol{x}}$ denotes the Jacobian operator (matrix) with respect to $\boldsymbol{x}$. The error expression then reduces to the following set of N equations with N unknowns:

$$\begin{cases} \dot{\boldsymbol{C}}_N^*(t) + \langle\boldsymbol{\Phi}_N,\boldsymbol{\Phi}_N\rangle_{\Omega}^{-1}\left(\langle\mathbf{J}_{\boldsymbol{x}}(\boldsymbol{\Phi}_N)\boldsymbol{f},\boldsymbol{\Phi}_N\rangle_{\Omega}\right. \\ \quad \left.-\frac{1}{4}\left[\sum_{\mathrm{k}=1}^{N} c_{\mathrm{k}}^*(t)\left\langle\mathbf{J}_{\boldsymbol{x}}(\boldsymbol{\Phi}_N)\boldsymbol{g}\boldsymbol{R}_{ct}^{-1}\boldsymbol{g}^{\mathrm{T}}\frac{\partial\phi_{\mathrm{k}}}{\partial\boldsymbol{x}},\boldsymbol{\Phi}_N\right\rangle_{\Omega}\right]\right)\boldsymbol{C}_N^*(t) \\ \quad +\langle\boldsymbol{\Phi}_N,\boldsymbol{\Phi}_N\rangle_{\Omega}^{-1}\langle l_{ct},\boldsymbol{\Phi}_N\rangle_{\Omega} = \boldsymbol{0} \\ \\ \boldsymbol{C}_N^*(t_{\mathrm{f}}) = \boldsymbol{0} \end{cases} \tag{29}$$

The following set of nonlinear ordinary differential equations termed *the continuous-time optimal control gain equations* needs therefore to be solved for $\boldsymbol{C}_N^*(t)$ in order to find the continuous-time optimal control law, assuming the equations have no escape in finite-time:

$$\dot{\boldsymbol{C}}_N^*(t) + \boldsymbol{A}(t,c_{\mathrm{k}}^*(t))\boldsymbol{C}_N^*(t) + \boldsymbol{b} = \boldsymbol{0} \quad , \quad \boldsymbol{C}_N^*(t_{\mathrm{f}}) = \boldsymbol{0} \tag{30}$$

where

$$\begin{aligned} \boldsymbol{M}(t,c_{\mathrm{k}}^*(t)) &= \sum_{\mathrm{k}=1}^{N} c_{\mathrm{k}}^*(t)\left\langle\mathbf{J}_{\boldsymbol{x}}(\boldsymbol{\Phi}_N)\boldsymbol{g}\boldsymbol{R}_{ct}^{-1}\boldsymbol{g}^{\mathrm{T}}\frac{\partial\phi_{\mathrm{k}}}{\partial\boldsymbol{x}},\boldsymbol{\Phi}_N\right\rangle_{\Omega} \\ \boldsymbol{A}(t,c_{\mathrm{k}}^*(t)) &= \langle\boldsymbol{\Phi}_N,\boldsymbol{\Phi}_N\rangle_{\Omega}^{-1}\left[\langle\mathbf{J}_{\boldsymbol{x}}(\boldsymbol{\Phi}_N)\boldsymbol{f},\boldsymbol{\Phi}_N\rangle_{\Omega} - \tfrac{1}{4}\boldsymbol{M}(t,c_{\mathrm{k}}^*(t))\right] \\ \boldsymbol{b} &= \langle\boldsymbol{\Phi}_N,\boldsymbol{\Phi}_N\rangle_{\Omega}^{-1}\langle l_{ct},\boldsymbol{\Phi}_N\rangle_{\Omega} \end{aligned} \tag{31}$$

Once the optimal control gains, $\boldsymbol{C}_N^*(t)$, are computed via backward integration of (30), the continuous-time optimal control law can be obtained by:

$$\boldsymbol{u}_{ct}^*(\boldsymbol{x}\,,\,t) = -\frac{1}{2}\boldsymbol{R}_{ct}^{-1}\boldsymbol{g}^{\mathrm{T}}(\boldsymbol{x}\,,\,t)\mathbf{J}_{\boldsymbol{x}}^{\mathrm{T}}(\boldsymbol{\Phi}_N(\boldsymbol{x}))\boldsymbol{C}_N^*(t) \tag{32}$$

In summary, starting with $\boldsymbol{f}$, $\boldsymbol{g}$, l_{ct}, $\boldsymbol{R}_{ct}$, $\boldsymbol{\Phi}_N$, and Ω as input, some definite n-dimensional integrals are first computed over a stability region defined by Ω. A nonlinear set of differential equations is then integrated backward in time using a fixed-step numerical scheme like fourth-order Runge–Kutta solver, RK4 (Quarteroni et al., 2000), to compute the optimal control gains, and the continuous-time nonlinear optimal control law is finally obtained as the output of the algorithm.

It should be noted that this algorithm can be used alone to synthesise optimal feedback controllers for the continuous-time finite-time horizon nonlinear systems (See section 4.1 and Sharifi & Damaren, 2020a).

2.2 Numerical solution to the discrete-time HJB equation

With the continuous-time optimal control gain equations, (30), thus derived, a set of algebraic equations is developed in this section to be solved for the optimal control gain vector associated with each jump at $t = t_k$. With the discrete-time dynamics (20) in mind, the impulsive Hamiltonian can be rewritten as below:

$$\begin{aligned} \mathcal{H}_{ds}(\boldsymbol{x}_k^-,\boldsymbol{u}_{ds,k},V(\boldsymbol{x},t_k),t_k) &= L_{ds}(\boldsymbol{x}_k^-,\boldsymbol{u}_{ds,k},t_k) + V(\boldsymbol{x}_k^+,t_k^+) \\ &\quad - V(\boldsymbol{x}_k^-,t_k^-) \end{aligned} \tag{33}$$

wherein $\boldsymbol{x}_k^{\pm} \triangleq \boldsymbol{x}(t_k^{\pm})$, and $V(\boldsymbol{x}_k^+,t_k^+) = V(\boldsymbol{x}_k^- + \boldsymbol{B}_{ds}\boldsymbol{u}_{ds,k},t_k^+)$. Defining $L_{ds} = l_{ds}(\boldsymbol{x}_k^-) + ||\boldsymbol{u}_{ds,k}||_{\boldsymbol{R}_{ds}}^2$, the discrete-time HJB equation, (6), at $t = t_k$ can be expressed as:

$$\begin{aligned} \min_{\boldsymbol{u}_{ds,k}\in\mathcal{U}_{ds}}\{&l_{ds}(\boldsymbol{x}_k^-) + ||\boldsymbol{u}_{ds,k}||_{\boldsymbol{R}_{ds}}^2 \\ &+ V(\boldsymbol{x}_k^- + \boldsymbol{B}_{ds}\boldsymbol{u}_{ds,k},t_k^+) - V(\boldsymbol{x}_k^-,t_k^-)\} = 0 \end{aligned} \tag{34}$$

wherein $l_{ds}:\mathcal{D}\to\mathbb{R}$ is the discrete-time state penalty function, and $\boldsymbol{R}_{ds}\in\mathbb{R}^{m_{ds}\times m_{ds}}$ denotes a symmetric positive-definite matrix called the discrete-time control penalty matrix. Minimising (34) with respect to $\boldsymbol{u}_{ds,k}$, the discrete-time optimal control

law, $\boldsymbol{u}^*_{ds,k}$, is therefore obtained by:

$$\begin{aligned}\boldsymbol{u}^*_{ds,k} &= -\frac{1}{2}\boldsymbol{R}_{ds}^{-1}\boldsymbol{B}_{ds}^{\mathrm{T}}\frac{\partial V(\boldsymbol{x}_k^+, t_k^+)}{\partial \boldsymbol{x}} \\ &= -\frac{1}{2}\boldsymbol{R}_{ds}^{-1}\boldsymbol{B}_{ds}^{\mathrm{T}}\frac{\partial V(\boldsymbol{x}_k^- + \boldsymbol{B}_{ds}\boldsymbol{u}^*_{ds,k}, t_k^+)}{\partial \boldsymbol{x}}\end{aligned} \tag{35}$$

Armed with the discrete-time optimal control law in terms of $V(\boldsymbol{x}_k, t_k)$, (35), and due to the fact that $\boldsymbol{u}^*_{ds,k}$ solves the impulsive optimal control problem (8), the discrete-time HJB equation in terms of $\boldsymbol{x}_k^-$ can be accordingly formulated by substituting (35) into (34):

$$\begin{aligned}\mathrm{HJB}_{ds}(V) = l_{ds}(\boldsymbol{x}_k^-) &+ \frac{1}{4}\left(\frac{\partial V(\boldsymbol{x}_k^- + \boldsymbol{B}_{ds}\boldsymbol{u}^*_{ds,k}, t_k^+)}{\partial \boldsymbol{x}}\right)^{\mathrm{T}} \\ &\times \boldsymbol{B}_{ds}\boldsymbol{R}_{ds}^{-1}\boldsymbol{B}_{ds}^{\mathrm{T}}\frac{\partial V(\boldsymbol{x}_k^- + \boldsymbol{B}_{ds}\boldsymbol{u}^*_{ds,k}, t_k^+)}{\partial \boldsymbol{x}} \\ &+ V(\boldsymbol{x}_k^- + \boldsymbol{B}_{ds}\boldsymbol{u}^*_{ds,k}, t_k^+) - V(\boldsymbol{x}_k^-, t_k^-) = 0\end{aligned} \tag{36}$$

Next, the truncated version of the discretized value function, (25), is substituted into (36) to obtain the following set of algebraic equations at each jump instant, $t = t_k$:

$$\begin{aligned}l_{ds}(\boldsymbol{x}_k^-) &+ \frac{1}{4}[\mathbf{J}_{\boldsymbol{x}}^{\mathrm{T}}(\boldsymbol{\Phi}_N(\boldsymbol{x}))|_{\boldsymbol{x}=\boldsymbol{x}_k^- + \boldsymbol{B}_{ds}\boldsymbol{u}^*_{ds,k}}\boldsymbol{C}_N^*(t_k^+)]^{\mathrm{T}}\boldsymbol{B}_{ds} \\ &\times \boldsymbol{R}_{ds}^{-1}\boldsymbol{B}_{ds}^{\mathrm{T}}[\mathbf{J}_{\boldsymbol{x}}^{\mathrm{T}}(\boldsymbol{\Phi}_N(\boldsymbol{x}))|_{\boldsymbol{x}=\boldsymbol{x}_k^- + \boldsymbol{B}_{ds}\boldsymbol{u}^*_{ds,k}}\boldsymbol{C}_N^*(t_k^+)] \\ &+ \boldsymbol{\Phi}_N^{\mathrm{T}}(\boldsymbol{x}_k^- + \boldsymbol{B}_{ds}\boldsymbol{u}^*_{ds,k})\boldsymbol{C}_N^*(t_k^+) - \boldsymbol{\Phi}_N^{\mathrm{T}}(\boldsymbol{x}_k^-)\boldsymbol{C}_N^*(t_k^-) = 0\end{aligned} \tag{37}$$

Having the knowledge of $\boldsymbol{C}_N^*(t_k^+)$ available from the backward integration of the continuous-time optimal control gain equations, (30), $\boldsymbol{C}_N^*(t_k^-)$ can be computed through the preceding set of equations. With the discrete-time optimal control gain equations, (37), thus derived, there are two main avenues of further formulation to approximate two unknown quantities at each jump instant, namely $\boldsymbol{x}_k^-$ and $\boldsymbol{u}^*_{ds,k}$. The former is handled through collocating $\boldsymbol{x}_k^-$ with a suitable set of points, $\bar{\boldsymbol{x}} = \underset{m}{\mathrm{row}}\{\bar{\boldsymbol{x}}_m\} = [\bar{\boldsymbol{x}}_1, \ \ldots \ , \ \bar{\boldsymbol{x}}_N]_{n\times N}$, while the latter is dealt with by defining the following function (via substituting (25) into (35) and then rearranging the resulting equation) in terms of $\boldsymbol{u}^*_{ds,k}$ and $\boldsymbol{x}_k^-$ with known quantities $c_j^*(t_k^+)$, and employing an appropriate numerical scheme to solve the resulting nonlinear set of algebraic equations for $\boldsymbol{u}^*_{ds,k}$:

$$\boldsymbol{F}(\boldsymbol{u}^*_{ds,k}) = 2\boldsymbol{R}_{ds}\boldsymbol{u}^*_{ds,k} + \boldsymbol{B}_{ds}^{\mathrm{T}}\sum_{j=1}^{N} c_j^*(t_k^+)\frac{\partial \phi_j(\boldsymbol{x}_k^- + \boldsymbol{B}_{ds}\boldsymbol{u}^*_{ds,k})}{\partial \boldsymbol{x}} = \boldsymbol{0} \tag{38}$$

The required tools are now in place to solve the discrete-time optimal control gain equations, (37), for $\boldsymbol{C}_N^*(t_k^-)$. To this end, Newton's method (Quarteroni et al., 2000) is employed to iteratively solve the equation $\boldsymbol{F}(\boldsymbol{u}^*_{ds,k}) = \boldsymbol{0}$ for $\boldsymbol{u}^{*(i+1)}_{ds,k}$, starting with $\boldsymbol{u}^{*(i)}_{ds,k}$:

$$\boldsymbol{u}^{*(i+1)}_{ds,k} = \boldsymbol{u}^{*(i)}_{ds,k} - \left(\frac{\partial \boldsymbol{F}(\boldsymbol{u}^{*(i)}_{ds,k})}{\partial \boldsymbol{u}^{*\mathrm{T}}_{ds,k}}\right)^{-1}\boldsymbol{F}(\boldsymbol{u}^{*(i)}_{ds,k}) \tag{39}$$

Substituting (38) into (39) along with use of chain rule yields:

$$\begin{aligned}\boldsymbol{u}^{*(i+1)}_{ds,k} = \boldsymbol{u}^{*(i)}_{ds,k} &- \left(2\boldsymbol{R}_{ds} + \boldsymbol{B}_{ds}^{\mathrm{T}}\sum_{j=1}^{N} c_j^*(t_k^+)\mathbf{H}_{\boldsymbol{x}}(\phi_j(\boldsymbol{x}))|_{\boldsymbol{x}=\boldsymbol{\chi}_k^+}\boldsymbol{B}_{ds}\right)^{-1} \\ &\times (2\boldsymbol{R}_{ds}\boldsymbol{u}^{*(i)}_{ds,k} + \boldsymbol{B}_{ds}^{\mathrm{T}}\mathbf{J}_{\boldsymbol{x}}^{\mathrm{T}}(\boldsymbol{\Phi}_N(\boldsymbol{x}))|_{\boldsymbol{x}=\boldsymbol{\chi}_k^+}\boldsymbol{C}_N^*(t_k^+))\end{aligned} \tag{40}$$

wherein $\boldsymbol{\chi}_k^+ = \boldsymbol{x}_k^- + \boldsymbol{B}_{ds}\boldsymbol{u}^{*(i)}_{ds,k}$, and $\mathbf{H}_{\boldsymbol{x}}$ is the Hessian matrix with respect to $\boldsymbol{x}$.

At this juncture in the development, $\boldsymbol{x}_k^-$ at each jump instant is collocated with $\bar{\boldsymbol{x}}_m$, $m = 1, \ldots, N$, and (40) is rewritten as follows with $\boldsymbol{x}_k^- = \bar{\boldsymbol{x}}_m$:

$$\begin{aligned}\boldsymbol{u}^{*(i+1)}_{ds,k} = \boldsymbol{u}^{*(i)}_{ds,k} &- \left(2\boldsymbol{R}_{ds} + \boldsymbol{B}_{ds}^{\mathrm{T}}\sum_{j=1}^{N} c_j^*(t_k^+)\mathbf{H}_{\boldsymbol{x}}(\phi_j(\boldsymbol{x}))|_{\boldsymbol{x}=\boldsymbol{\chi}_{k,m}^+}\boldsymbol{B}_{ds}\right)^{-1} \\ &\times (2\boldsymbol{R}_{ds}\boldsymbol{u}^{*(i)}_{ds,k} + \boldsymbol{B}_{ds}^{\mathrm{T}}\mathbf{J}_{\boldsymbol{x}}^{\mathrm{T}}(\boldsymbol{\Phi}_N(\boldsymbol{x}))|_{\boldsymbol{x}=\boldsymbol{\chi}_{k,m}^+}\boldsymbol{C}_N^*(t_k^+))\end{aligned} \tag{41}$$

where $\boldsymbol{\chi}_{k,m}^+ = \bar{\boldsymbol{x}}_m + \boldsymbol{B}_{ds}\boldsymbol{u}^{*(i)}_{ds,k}$, and the convergence criteria at each iteration can be defined as:

$$|\,||\boldsymbol{u}^{*(i+1)}_{ds,k}|| - ||\boldsymbol{u}^{*(i)}_{ds,k}||\,| < \varepsilon \qquad \text{or} \qquad ||\boldsymbol{F}(\boldsymbol{u}^{*(i)}_{ds,k})|| < \delta \tag{42}$$

wherein ε and δ are two sufficiently small positive arbitrary numbers.

Initialising (41) with a suitable choice of $\boldsymbol{u}^{*(0)}_{ds,k}$ (for instance $\boldsymbol{u}^{*(0)}_{ds,k} = \boldsymbol{0}$), the discrete-time optimal control corresponding to each $\bar{\boldsymbol{x}}_m$ at $t = t_k$, $\boldsymbol{u}^*_{ds,k}(\bar{\boldsymbol{x}}_m, t_k)$, can be therefore computed for $m = 1, \ldots, N$. Utilising the spectral collocation method at each jump instant and substituting $\boldsymbol{u}^*_{ds,k}(\bar{\boldsymbol{x}}_m, t_k)$ computed from (41) into (37), *the discrete-time optimal control gain equations* are ultimately obtained to be solved for $\boldsymbol{C}_N^*(t_k^-)$ as follows:

$$\boldsymbol{C}_N^*(t_k^-) = (\Psi_k^-(\bar{\boldsymbol{x}}))^{-1}[\boldsymbol{W}_k(\bar{\boldsymbol{x}}) + \Psi_k^+(\bar{\boldsymbol{x}})\boldsymbol{C}_N^*(t_k^+)] \tag{43}$$

where

$$\boldsymbol{\Upsilon}(\bar{\boldsymbol{x}}_m) = \mathbf{J}_{\boldsymbol{x}}^{\mathrm{T}}(\boldsymbol{\Phi}_N(\boldsymbol{x}))|_{\boldsymbol{x}=\bar{\boldsymbol{x}}_m+\boldsymbol{B}_{ds}\boldsymbol{u}^*_{ds,k}(\bar{\boldsymbol{x}}_m,t_k)}\, \boldsymbol{C}^*_N(t_k^+)$$

$$\boldsymbol{W}_k(\bar{\boldsymbol{x}}) = \underset{m}{\text{column}} \left\{ l_{ds}(\bar{\boldsymbol{x}}_m) + \frac{1}{4}(\Upsilon^{\mathrm{T}}(\bar{\boldsymbol{x}}_m)\boldsymbol{B}_{ds}\boldsymbol{R}_{ds}^{-1}\boldsymbol{B}_{ds}^{\mathrm{T}}\Upsilon(\bar{\boldsymbol{x}}_m)) \right\}$$
$$= \begin{bmatrix} l_{ds}(\bar{\boldsymbol{x}}_1) + \frac{1}{4}(\Upsilon^{\mathrm{T}}(\bar{\boldsymbol{x}}_1)\boldsymbol{B}_{ds}\boldsymbol{R}_{ds}^{-1}\boldsymbol{B}_{ds}^{\mathrm{T}}\Upsilon(\bar{\boldsymbol{x}}_1)) \\ \vdots \\ l_{ds}(\bar{\boldsymbol{x}}_N) + \frac{1}{4}(\Upsilon^{\mathrm{T}}(\bar{\boldsymbol{x}}_N)\boldsymbol{B}_{ds}\boldsymbol{R}_{ds}^{-1}\boldsymbol{B}_{ds}^{\mathrm{T}}\Upsilon(\bar{\boldsymbol{x}}_N)) \end{bmatrix}_{N\times 1}$$

$$\Psi_k^-(\bar{\boldsymbol{x}}) = \underset{m,j}{\text{matrix}}\{\phi_j(\bar{\boldsymbol{x}}_m)\} = \begin{bmatrix} \phi_1(\bar{\boldsymbol{x}}_1) & \cdots & \phi_N(\bar{\boldsymbol{x}}_1) \\ \vdots & \ddots & \vdots \\ \phi_1(\bar{\boldsymbol{x}}_N) & \cdots & \phi_N(\bar{\boldsymbol{x}}_N) \end{bmatrix}_{N\times N}$$

$$\Psi_k^+(\bar{\boldsymbol{x}}) = \underset{m,j}{\text{matrix}}\{\phi_j(\bar{\boldsymbol{x}}_m + \boldsymbol{B}_{ds}\boldsymbol{u}^*_{ds,k}(\bar{\boldsymbol{x}}_m,t_k))\}$$
$$= \begin{bmatrix} \phi_1(\bar{\boldsymbol{x}}_1 + \boldsymbol{B}_{ds}\boldsymbol{u}^*_{ds,k}(\bar{\boldsymbol{x}}_1,t_k)) & \cdots & \phi_N(\bar{\boldsymbol{x}}_1 + \boldsymbol{B}_{ds}\boldsymbol{u}^*_{ds,k}(\bar{\boldsymbol{x}}_1,t_k)) \\ \vdots & \ddots & \vdots \\ \phi_1(\bar{\boldsymbol{x}}_N + \boldsymbol{B}_{ds}\boldsymbol{u}^*_{ds,k}(\bar{\boldsymbol{x}}_N,t_k)) & \cdots & \phi_N(\bar{\boldsymbol{x}}_N + \boldsymbol{B}_{ds}\boldsymbol{u}^*_{ds,k}(\bar{\boldsymbol{x}}_N,t_k)) \end{bmatrix}_{N\times N} \tag{44}$$

To succinctly summarise, the discrete-time portion of the hybrid algorithm being proposed is initialised with $\boldsymbol{B}_{ds}$, l_{ds}, $\boldsymbol{R}_{ds}$, $\boldsymbol{Q}_{ds}$, and $\bar{\boldsymbol{x}}$ as input. Employing Newton's method to compute $\boldsymbol{u}^*_{ds,k}(\bar{\boldsymbol{x}}_m,t_k)$ at each jump instant, $\boldsymbol{C}^*_N(t_k^-)$ is then found through the discrete-time optimal control gain equations. In the final step, (40) fed by $\boldsymbol{x}_k^-$ and $\boldsymbol{C}^*_N(t_k^+)$ is evoked at each jump to obtain the discrete-time nonlinear optimal control as the output of the algorithm.

It must be noted that the system (19) and (20) are assumed to be controllable on $\Omega \times [t_0, t_f]$ throughout this paper.

2.2.1 Specialisation to the LQR case

In this section, the numerical scheme employed to solve the equation (38), and the proposed approach to drive the discrete-time optimal control gain equations are specialised to the LQR case to analytically evaluate the approaches being proposed. By defining $V(\boldsymbol{x},t) = \boldsymbol{x}^{\mathrm{T}}\boldsymbol{P}(t)\boldsymbol{x}$ corresponding to the LQR case, (38) can be written as:

$$\boldsymbol{F}(\boldsymbol{u}^*_{ds,k}) = 2\boldsymbol{R}_{ds}\boldsymbol{u}^*_{ds,k} + 2\boldsymbol{B}_{ds}^{\mathrm{T}}\boldsymbol{P}_k^+(\boldsymbol{x}_k^- + \boldsymbol{B}_{ds}\boldsymbol{u}^*_{ds,k}) = \boldsymbol{0} \tag{45}$$

where $\boldsymbol{P}(t)$ denotes the time-varying Riccati solution, and $\boldsymbol{P}_k^{\pm} \triangleq \boldsymbol{P}(t_k^{\pm})$. The proposed numerical scheme to solve (45), namely Newton's method, is therefore arranged as:

$$\boldsymbol{u}^{*(i+1)}_{ds,k} = \boldsymbol{u}^{*(i)}_{ds,k} - (\boldsymbol{R}_{ds} + \boldsymbol{B}_{ds}^{\mathrm{T}}\boldsymbol{P}_k^+\boldsymbol{B}_{ds})^{-1} \times [\boldsymbol{R}_{ds}\boldsymbol{u}^{*(i)}_{ds,k} + \boldsymbol{B}_{ds}^{\mathrm{T}}\boldsymbol{P}_k^+(\boldsymbol{x}_k^- + \boldsymbol{B}_{ds}\boldsymbol{u}^{*(i)}_{ds,k})] \tag{46}$$

As is evident, when (46) is initialised by a simple choice of $\boldsymbol{u}^{*(0)}_{ds,k} = \boldsymbol{0}$, the discrete-time optimal control law computed via the approximation converges to the discrete-time Riccati optimal control immediately after one iteration (i.e. $\boldsymbol{u}^*_{ds,k}$ is the exact solution when $V(\boldsymbol{x},t) = \boldsymbol{x}^{\mathrm{T}}\boldsymbol{P}(t)\boldsymbol{x}$):

$$\boldsymbol{u}^{*(1)}_{ds,k} = -[\boldsymbol{R}_{ds} + \boldsymbol{B}_{ds}^{\mathrm{T}}\boldsymbol{P}_k^+\boldsymbol{B}_{ds}]^{-1}\boldsymbol{B}_{ds}^{\mathrm{T}}\boldsymbol{P}_k^+\boldsymbol{x}_k^- \tag{47}$$

With $V(\boldsymbol{x},t) = \boldsymbol{x}^{\mathrm{T}}\boldsymbol{P}(t)\boldsymbol{x}$, the proposed approach to develop the discrete-time optimal control gain equations can be now assessed for the LQR case. In this regard, the discrete-time optimal control law, (35), can be simplified as $\boldsymbol{u}^*_{ds,k} = -\boldsymbol{R}_{ds}^{-1}\boldsymbol{B}_{ds}^{\mathrm{T}}\boldsymbol{P}_k^+(\boldsymbol{x}_k^- + \boldsymbol{B}_{ds}\boldsymbol{u}^*_{ds,k})$. Therefore:

$$\boldsymbol{u}^*_{ds,k} = -[\boldsymbol{R}_{ds} + \boldsymbol{B}_{ds}^{\mathrm{T}}\boldsymbol{P}_k^+\boldsymbol{B}_{ds}]^{-1}\boldsymbol{B}_{ds}^{\mathrm{T}}\boldsymbol{P}_k^+\boldsymbol{x}_k^- \tag{48}$$

which is the discrete-time Riccati optimal control law at $t = t_k$ (Sobiesiak & Damaren, 2015a). Choosing $l_{ds}(\boldsymbol{x}_k^-) = \boldsymbol{x}_k^{-\mathrm{T}}\boldsymbol{Q}_{ds}\boldsymbol{x}_k^-$, substitution of $V(\boldsymbol{x},t) = \boldsymbol{x}^{\mathrm{T}}\boldsymbol{P}(t)\boldsymbol{x}$ and (48) into (36) yields:

$$\boldsymbol{x}_k^{-\mathrm{T}}\boldsymbol{P}_k^+\boldsymbol{B}_{ds}[\boldsymbol{R}_{ds} + \boldsymbol{B}_{ds}^{\mathrm{T}}\boldsymbol{P}_k^+\boldsymbol{B}_{ds}]^{-\mathrm{T}}\boldsymbol{R}_{ds}[\boldsymbol{R}_{ds} + \boldsymbol{B}_{ds}^{\mathrm{T}}\boldsymbol{P}_k^+\boldsymbol{B}_{ds}]^{-1}\boldsymbol{B}_{ds}^{\mathrm{T}}\boldsymbol{P}_k^+\boldsymbol{x}_k^- + \boldsymbol{x}_k^{-\mathrm{T}}\boldsymbol{Q}_{ds}\boldsymbol{x}_k^- + \boldsymbol{x}_k^{+\mathrm{T}}\boldsymbol{P}_k^+\boldsymbol{x}_k^+ - \boldsymbol{x}_k^{-\mathrm{T}}\boldsymbol{P}_k^-\boldsymbol{x}_k^- = \boldsymbol{0} \tag{49}$$

The discrete-time optimal control gain equations are therefore reduced to:

$$\boldsymbol{P}_k^- = \boldsymbol{Q}_{ds} - \boldsymbol{P}_k^+\boldsymbol{B}_{ds}[\boldsymbol{R}_{ds} + \boldsymbol{B}_{ds}^{\mathrm{T}}\boldsymbol{P}_k^+\boldsymbol{B}_{ds}]^{-1}\boldsymbol{B}_{ds}^{\mathrm{T}}\boldsymbol{P}_k^+ + \boldsymbol{P}_k^+ \tag{50}$$

which are the discrete-time Riccati-based optimal control gain equations at $t = t_k$ (i.e. the optimal control gain vector at $t = t_k$ is the exact solution when $V(\boldsymbol{x},t) = \boldsymbol{x}^{\mathrm{T}}\boldsymbol{P}(t)\boldsymbol{x}$).

2.3 Hybrid nonlinear optimal control law

Armed with the continuous-time and discrete-time optimal control gain equations, (30) and (43) respectively, the desired hybrid nonlinear optimal control gains can be now computed at each time instant through solving the following sets of equations (known as *the hybrid optimal control gain equations*) for $\boldsymbol{C}^*_N(t)$:

$$\begin{cases} \dot{\boldsymbol{C}}^*_N(t) + \boldsymbol{A}(t, c^*_k(t))\boldsymbol{C}^*_N(t) + \boldsymbol{b} = \boldsymbol{0} \ , \ \boldsymbol{C}^*_N(t_f) = \boldsymbol{0} \\ \qquad (See\ (31)) \quad t \neq t_k \\ \boldsymbol{C}^*_N(t_k^-) = (\Psi_k^-(\bar{\boldsymbol{x}}))^{-1}[\boldsymbol{W}_k(\bar{\boldsymbol{x}}) + \Psi_k^+(\bar{\boldsymbol{x}})\boldsymbol{C}^*_N(t_k^+)] \\ \qquad (See\ (44)) \quad t = t_k \end{cases} \tag{51}$$

Starting with the boundary conditions at the terminal time, $\boldsymbol{C}^*_N(t_f) = \boldsymbol{0}$, the continuous-time optimal control gain equations are first integrated backward in time to compute $\boldsymbol{C}^*_N(t)$ between impulsive instants. At each jump instant, $t = t_k$, an impulse is then induced in the solution using the discrete-time optimal control gain equations, and $\boldsymbol{C}^*_N(t_k^-)$ computed at each jump is subsequently used as a new set of terminal conditions for the continuous-time optimal control gain equations to be integrated backward from t_k^- to t_{k-1}^+. This integration process is repeated until time zero is reached.

With the hybrid nonlinear optimal control gain vector thus computed at each time instant, the hybrid nonlinear optimal control law can be ultimately found by:

$$\begin{cases} \boldsymbol{u}^*_{ct}(\boldsymbol{x}\,,\,t) = -\frac{1}{2}\boldsymbol{R}_{ct}^{-1}\boldsymbol{g}^{\mathrm{T}}(\boldsymbol{x}\,,\,t)\mathbf{J}_{\boldsymbol{x}}^{\mathrm{T}}(\boldsymbol{\Phi}_N(\boldsymbol{x}))\boldsymbol{C}^*_N(t) \quad t \neq t_k \\ \boldsymbol{u}^*_{ds,k}(\boldsymbol{x}_k^+\,,\,t_k^+) = -\frac{1}{2}\boldsymbol{R}_{ds}^{-1}\boldsymbol{B}_{ds}^{\mathrm{T}}\mathbf{J}_{\boldsymbol{x}}^{\mathrm{T}}(\boldsymbol{\Phi}_N(\boldsymbol{x}))|_{\boldsymbol{x}=\boldsymbol{x}_k^+}\boldsymbol{C}^*_N(t_k^+) \quad t = t_k \end{cases} \tag{52}$$

Shown in Figure 1, the proposed hybrid algorithm for nonlinear systems is compared to the hybrid LQR approach (Sobiesiak

Hybrid Nonlinear Optimal Control	*Hybrid Riccati-based Optimal (LQR) Control*
$\begin{cases} \dot{\boldsymbol{x}} = \boldsymbol{f}(\boldsymbol{x},t) + \boldsymbol{g}(\boldsymbol{x},t)\boldsymbol{u}_{ct}(\boldsymbol{x},t) & t \neq t_k \\ \boldsymbol{x}_k^+ = \boldsymbol{x}_k^- + \boldsymbol{B}_{ds}\boldsymbol{u}_{ds,k} & t = t_k \end{cases}, \ \boldsymbol{x}(\boldsymbol{0}) = \boldsymbol{x}_0$	$\begin{cases} \dot{\boldsymbol{x}} = \boldsymbol{A}_{ct}(t)\boldsymbol{x} + \boldsymbol{B}_{ct}(t)\boldsymbol{u}_{ct}(\boldsymbol{x},t) & t \neq t_k \\ \boldsymbol{x}_k^+ = \boldsymbol{x}_k^- + \boldsymbol{B}_{ds}\boldsymbol{u}_{ds,k} & t = t_k \end{cases}, \ \boldsymbol{x}(\boldsymbol{0}) = \boldsymbol{x}_0$
$V_N(\boldsymbol{x},t) := \sum_{j=1}^{N} c_j^*(t)\,\phi_j(\boldsymbol{x}) = \boldsymbol{\Phi}_N^{\mathrm{T}}(\boldsymbol{x})\boldsymbol{C}_N^*(t)$	$V(\boldsymbol{x},t) := \boldsymbol{x}^{\mathrm{T}}\boldsymbol{P}(t)\boldsymbol{x}$
$J(\boldsymbol{x},\boldsymbol{u}_{ct},\boldsymbol{u}_{ds,k},t) = \int_{t_0}^{t_f}\left(l_{ct}(\boldsymbol{x}) + \left\|\boldsymbol{u}_{ct}\right\|_{\boldsymbol{R}_{ct}}^2\right)dt + \sum_{k=1}^{N_{imp}}\left(l_{ds}(\boldsymbol{x}_k^-) + \left\|\boldsymbol{u}_{ds,k}\right\|_{\boldsymbol{R}_{ds}}^2\right)$	$J(\boldsymbol{x},\boldsymbol{u}_{ct},\boldsymbol{u}_{ds,k},t) = \int_{t_0}^{t_f}(\boldsymbol{x}^{\mathrm{T}}\boldsymbol{Q}_{ct}\boldsymbol{x} + \boldsymbol{u}_{ct}^{\mathrm{T}}\boldsymbol{R}_{ct}\boldsymbol{u}_{ct})\,dt + \sum_{k=1}^{N_{imp}}(\boldsymbol{x}_k^{-\mathrm{T}}\boldsymbol{Q}_{ds}\boldsymbol{x}_k^- + \boldsymbol{u}_{ds,k}^{\mathrm{T}}\boldsymbol{R}_{ds}\boldsymbol{u}_{ds,k})$
$\begin{cases} \dot{\boldsymbol{C}}_N^*(t) + \boldsymbol{A}\left(t, c_{\mathrm{k}}^*(t)\right)\boldsymbol{C}_N^*(t) + \boldsymbol{b} = \boldsymbol{0}\ ,\ \boldsymbol{C}_N^*(t_{\mathrm{f}}) = \boldsymbol{0} & \\ See\,(31) & t \neq t_k \\ \boldsymbol{C}_N^*(t_k^-) = \left(\boldsymbol{\Psi}_k^-(\bar{\boldsymbol{x}})\right)^{-1}\left[\boldsymbol{W}_k(\bar{\boldsymbol{x}}) + \boldsymbol{\Psi}_k^+(\bar{\boldsymbol{x}})\boldsymbol{C}_N^*(t_k^+)\right] & \\ See\,(44) & t = t_k \end{cases}$	$\begin{cases} \dot{\boldsymbol{P}}(t) + \boldsymbol{A}_{ct}^{\mathrm{T}}\boldsymbol{P}(t) + \boldsymbol{P}(t)\boldsymbol{A}_{ct} + \boldsymbol{Q}_{ct} & \\ -\boldsymbol{P}(t)\boldsymbol{B}_{ct}\boldsymbol{R}_{ct}^{-1}\boldsymbol{B}_{ct}^{\mathrm{T}}\boldsymbol{P}(t) = \boldsymbol{0}\ ,\ \boldsymbol{P}(t_{\mathrm{f}}) = \boldsymbol{0} & t \neq t_k \\ \boldsymbol{P}_k^- = \boldsymbol{Q}_{ds} + \boldsymbol{P}_k^+ & \\ \quad -\boldsymbol{P}_k^+\boldsymbol{B}_{ds}\left[\boldsymbol{R}_{ds} + \boldsymbol{B}_{ds}^{\mathrm{T}}\boldsymbol{P}_k^+\boldsymbol{B}_{ds}\right]^{-1}\boldsymbol{B}_{ds}^{\mathrm{T}}\boldsymbol{P}_k^+ & t = t_k \end{cases}$
$\boldsymbol{C}_N^*(t)$	$\boldsymbol{P}(t)$
$\begin{cases} \boldsymbol{u}_{ct}^* = -\frac{1}{2}\boldsymbol{R}_{ct}^{-1}\boldsymbol{g}^{\mathrm{T}}(\boldsymbol{x},t)\mathbf{J}_{\boldsymbol{x}}^{\mathrm{T}}\left(\boldsymbol{\Phi}_N(\boldsymbol{x})\right)\boldsymbol{C}_N^*(t) & t \neq t_k \\ \boldsymbol{u}_{ds,k}^* = -\frac{1}{2}\boldsymbol{R}_{ds}^{-1}\boldsymbol{B}_{ds}^{\mathrm{T}}\,\mathbf{J}_{\boldsymbol{x}}^{\mathrm{T}}\left(\boldsymbol{\Phi}_N(\boldsymbol{x})\right)\big\|_{\boldsymbol{x}=\boldsymbol{x}_k^+}\boldsymbol{C}_N^*(t_k^+) & t = t_k \end{cases}$	$\begin{cases} \boldsymbol{u}_{ct}^* = -\boldsymbol{R}_{ct}^{-1}\boldsymbol{B}_{ct}^{\mathrm{T}}(t)\boldsymbol{P}(t)\boldsymbol{x} & t \neq t_k \\ \boldsymbol{u}_{ds,k}^* = -\boldsymbol{R}_{ds}^{-1}\boldsymbol{B}_{ds}^{\mathrm{T}}\left[\boldsymbol{P}_k^- - \boldsymbol{Q}_{ds}\right]\boldsymbol{x}_k^- & t = t_k \end{cases}$

Figure 1. Comparison between the proposed hybrid nonlinear optimal control (left) and the hybrid Riccati-based (LQR) control (right).

& Damaren, 2015a) applicable for linear systems wherein $V(\boldsymbol{x},\,t) := \boldsymbol{x}^{\mathrm{T}}\boldsymbol{P}(t)\boldsymbol{x}$. Defining $(\boldsymbol{x}_{eq}, \boldsymbol{u}_{eq})$ as desired equilibrium for the hybrid dynamical system being considered, the dynamic and control input matrices for the LQR case shown in Figure 1 can be respectively found by:

$$\begin{aligned} \boldsymbol{A}_{ct}(t) &= \mathbf{J}_{\boldsymbol{x}}(\boldsymbol{F}_{ct}(\boldsymbol{x},\boldsymbol{u}_{ct},t))|_{\boldsymbol{x}=\boldsymbol{x}_{eq},\,\boldsymbol{u}_{ct}=\boldsymbol{u}_{eq}} \\ \boldsymbol{B}_{ct}(t) &= \mathbf{J}_{\boldsymbol{u}_{ct}}(\boldsymbol{F}_{ct}(\boldsymbol{x},\boldsymbol{u}_{ct},t))|_{\boldsymbol{x}=\boldsymbol{x}_{eq},\,\boldsymbol{u}_{ct}=\boldsymbol{u}_{eq}} \end{aligned} \tag{53}$$

As opposed to the LQR method wherein the state penalty functions must be necessarily quadratic, $l_{ct}(\boldsymbol{x})$ and $l_{ds}(\boldsymbol{x}_k^-)$ in the proposed nonlinear approach can be any positive-definite function of $\boldsymbol{x}$; although they are commonly chosen to be quadratic.

3. Practical considerations

Given the dynamics and a performance index for a hybrid nonlinear dynamical system, three major parameters must be appropriately chosen to apply the proposed hybrid algorithm:

- A compact set that contains the origin as an interior point and is preferably symmetric about it,
- A set of basis functions that can adequately approximate the value function, and
- A set of collocation points that locates inside and on the boundaries of the compact set.

The compact set (or stability region or a bounded domain of the state space), Ω, is defined as the domain of possible values for the states. Ω can be determined according to some physical, kinematical or practical limitations (physical capabilities) of the system, and the likely deviation of the system states from their nominal value of zero (Beard, 1995). For instance, when an attitude control problem using Gibbs parameters is concerned, the domain of the state space for Gibbs parameters should be around $[-3, 3]$ radians because the singularities associated with Gibbs parameters occur at $-\pi$ and π. For angular velocity components, however, there is no kinematical limitation; their stability region can be therefore chosen on the basis of practical considerations.

The proper selection of basis functions is critical to the design of the nonlinear optimal controllers. Two important requirements, namely characteristic and quantity, must be satisfied in order to make an appropriate choice of basis functions. For the control to compensate adequately for the nonlinear dynamics of the system, basis functions must be able to capture the essential nonlinear dynamics of the system. If the system has dynamics that are not spanned by the basis functions, then the control will not be able to compensate for the dynamics of the

system (*characteristic requirement*) (Beard, 1995; Beard et al., 1996). The number of basis elements must also be sufficiently large to approximate the value function with sufficient accuracy (*quantity requirement*) (Beard, 1995; Beard et al., 1996). Therefore, the accuracy of V_N depends on the characteristics and quantities of the basis elements chosen to form the approximation.

As demonstrated in Beard (1995), polynomials are proven to work very well as basis functions in this algorithm. To the knowledge of the current authors, the best way to find an appropriate choice of basis functions for finite-time horizon systems is to start with the quadratic basis elements obtained by the second-order expansion of the states, eliminating those terms whose corresponding control gains are either zero or very small as compared to the other terms. The remaining basis elements (*effective quadratic terms*) are then augmented by some extra higher-order terms to capture the essential nonlinear dynamics of the system, and to improve the performance of the system. Due to multiplication of $\boldsymbol{g}^{\mathrm{T}}(\boldsymbol{x}, t)$ and $\boldsymbol{J}_{\boldsymbol{x}}^{\mathrm{T}}(\boldsymbol{\Phi}_N(\boldsymbol{x}))$ in the continuous-time optimal control law, (32), these extra higher-order basis elements must be selected such that their partial derivatives with respect to those states which correspond to non-zero elements of $\boldsymbol{g}(\boldsymbol{x}, t)$ in (32) result in desired functions of the states to ultimately appear in the optimal control law, hence capture the dominant nonlinear dynamics of the system. For clarification, consider a four-dimensional system with the following control input function:

$$\boldsymbol{g}(\boldsymbol{x}, t) = \begin{bmatrix} 0 & 0 & g_{31} & 0 \\ 0 & 0 & 0 & g_{42} \end{bmatrix}^{\mathrm{T}}$$

where $\boldsymbol{x} = \begin{bmatrix} x_1 & x_2 & x_3 & x_4 \end{bmatrix}^{\mathrm{T}}$, and g_{31} and g_{42} represent the non-zero elements of $\boldsymbol{g}$. In this case, any basis element consisting of either x_3 or x_4 associated with g_{31} and g_{42} respectively will show up in the optimal control law as follows:

$$\begin{aligned}
\boldsymbol{u}_{ct}^*(\boldsymbol{x}, t) &= -\frac{1}{2}\boldsymbol{R}_{ct}^{-1}\boldsymbol{g}^{\mathrm{T}}\boldsymbol{J}_{\boldsymbol{x}}^{\mathrm{T}}(\boldsymbol{\Phi}_N(\boldsymbol{x}))\boldsymbol{C}_N^*(t) \\
&= -\frac{1}{2}\boldsymbol{R}_{ct}^{-1}\begin{bmatrix} 0 & 0 & g_{31} & 0 \\ 0 & 0 & 0 & g_{42} \end{bmatrix}\begin{bmatrix} \frac{\partial\phi_1}{\partial x_1} & \cdots & \frac{\partial\phi_N}{\partial x_1} \\ \vdots & & \vdots \\ \frac{\partial\phi_1}{\partial x_4} & \cdots & \frac{\partial\phi_N}{\partial x_4} \end{bmatrix} \\
&\quad \times \begin{bmatrix} c_1^*(t) \\ \vdots \\ c_N^*(t) \end{bmatrix} \\
&= -\frac{1}{2}\boldsymbol{R}_{ct}^{-1}\begin{bmatrix} g_{31}\frac{\partial\phi_1}{\partial x_3} & \cdots & g_{31}\frac{\partial\phi_N}{\partial x_3} \\ g_{42}\frac{\partial\phi_1}{\partial x_4} & \cdots & g_{42}\frac{\partial\phi_N}{\partial x_4} \end{bmatrix}\begin{bmatrix} c_1^*(t) \\ \vdots \\ c_N^*(t) \end{bmatrix}
\end{aligned}$$

Extra higher-order basis elements must be therefore chosen such that their partial derivatives with respect to x_3 and x_4 give rise to some desired functions of $\boldsymbol{x}$ to ultimately emerge in the optimal control law, and consequently capture the significant nonlinear dynamics of the system. For example, if the dynamics consist of a nonlinear term like $x_1^2x_2$, basis elements of the form $x_1^2x_2x_3$ or $x_1^2x_2x_4$ (or even $x_1^2x_2x_3x_4$) will eventually produce $x_1^2x_2$ in the optimal control law to capture the nonlinear terms involved in the dynamics.

By increasing the number of basis elements in a manner consistent with the characteristic requirement, V_N gradually approaches to V. At a certain number of basis elements, the hybrid performance index is ultimately converged, i.e. $V_N \cong V$, and the quantity requirement is accordingly met. Henceforth, any further increase in the number of basis elements yields insignificant improvement in the performance index at the expense of computational cost. This process requires a deep understanding of the dynamical behaviour of the system, as well as trial and error. In addition to characteristic and quantity requirements stressed above, an appropriate choice of basis functions must also produce an invertible $\langle \boldsymbol{\Phi}_N, \boldsymbol{\Phi}_N \rangle_\Omega$ matrix.

It should be noted that the optimal control law (32) can be linear or nonlinear depending upon the structure of the function $\boldsymbol{g}$ and the characteristics of the basis elements. If $\boldsymbol{g}$ is only constant or time-dependent, (32) is linear if the basis functions are only constructed by quadratic terms, and nonlinear if $\boldsymbol{\Phi}_N$ contains extra higher-order terms as well. However, if $\boldsymbol{g}$ is state-dependent, whether time-dependent or not, (32) might be nonlinear even if $\boldsymbol{\Phi}_N$ only contains quadratic terms depending on the structure of $\boldsymbol{g}$.

A suitable set of collocation points is also necessary to design the discrete-time optimal controller. Collocation points can be chosen from the entire compact set excluding the origin, provided the rank condition required to produce an invertible $\Psi_k^-(\bar{\boldsymbol{x}})$ in (43) is satisfied. Although this rank test is the only requirement for any set of collocation points to be admissible, for those systems whose discrete-time control penalty matrix, $\boldsymbol{R}_{ds}$, is desired to be minimum (to apply the largest possible impulsive thrusts), a condition number test is also recommended. By performing this condition number test, a choice of $\bar{\boldsymbol{x}}$, amongst all available candidates satisfying the rank requirement, which produces the smallest possible condition number for $\Psi_k^-(\bar{\boldsymbol{x}})$ is obtained. This choice expands the acceptable range of $\boldsymbol{R}_{ds}$ from lower bound ($\boldsymbol{R}_{ds}$ in the denominator of (41) must be sufficiently large for the equation to converge) and makes it possible to choose a smaller $\boldsymbol{R}_{ds}$ as necessary.

As might be expected, the main drawback associated with this approach is the curse of dimensionality. Depending upon the dimension of the state space of the system, n, the calculation of the optimal control gains, $\boldsymbol{C}_N^*(t)$, can be computationally demanding. However, there are numerous options to deal effectively with the dimensionality problem. First of all, through judicious selection of basis functions, the curse of dimensionality can be significantly mitigated. For instance, under certain conditions, the characteristics of the basis elements can be confined to even polynomials in the states (Beard et al., 1997). In addition, the structure of the algorithm can be exploited to reduce the amount of computations from exponential to polynomial growth in the dimension of the state space (Beard & McLain, 1998b; Lawton & Beard, 1998). For example, if the system equations are separable, and Ω is symmetric about the origin, then the n-dimensional integrals reduce to iterated one-dimensional ones (Beard et al., 1996; Beard & McLain, 1998b). As another example, if the penalty functions involved in the algorithm are defined to be quadratic, the weighting matrices corresponding to both state and control penalty functions can be taken outside the integral, thereby tuning the system computationally fast (Beard et al., 1997). Moreover, symbolic software

is recommended to use for further alleviation of the computational cost associated with the integrations (Beard, 1995).

Lastly, all computations involved in the algorithm are performed off-line (prior to implementation); once the optimal control gains, $\boldsymbol{C}_N^*(t)$, are determined through numerically solving (51), the optimal control architecture can be implemented in hardware and run in real time. However, there are some possibilities to facilitate the implementation of the proposed hybrid controller. For instance, assuming a periodic or quasi-periodic nature for the optimal control gains over the operating time, Fourier series (Boyce & DiPrima, 1992) can be employed to approximate the steady-state part of $\boldsymbol{C}_N^*(t)$ by discarding the initial transient phase coming backward from t_f (See section V in Sharifi & Damaren, 2020a as an example). Rather than storing the entire time history of $\boldsymbol{C}_N^*(t)$, the Fourier coefficients associated with Fourier-based approximation can be stored onboard. As a consequence, not only the storage memory requirement is significantly reduced, but also $\boldsymbol{C}_N^*(t)$ is no longer restricted to the time interval from 0 to t_f (defined by user for control design), and can be extended to any desired operating time. However, the number of coefficients in Fourier series must be sufficiently large to accurately capture the actual periodic part of $\boldsymbol{C}_N^*(t)$.

4. Illustrative examples

This section serves to evaluate the functionality of the proposed control design framework through two examples. The first example is a one-dimensional continuous-time linear system for which it is easy to find the actual optimal solution. Therefore, the results obtained by the approximation can be compared to the exact optimal solution, thereby evaluating the algorithm proposed in section 2.1. The second example demonstrates the applicability of the proposed hybrid algorithm summarised in Figure 1 for a four-dimensional system. In both examples, a fixed-step fourth-order Runge–Kutta scheme (RK4) is used to integrate the differential equations backward and forward in time. In addition, the state penalty functions are chosen to be quadratic for both examples:

$$l_{ct}(\boldsymbol{x}) = \boldsymbol{x}^{\mathrm{T}}\boldsymbol{Q}_{ct}\boldsymbol{x} \quad , \quad l_{ds}(\boldsymbol{x}_k^-) = \boldsymbol{x}_k^{-\mathrm{T}}\boldsymbol{Q}_{ds}\boldsymbol{x}_k^-$$

where $\boldsymbol{Q}_{ct}$ and $\boldsymbol{Q}_{ds}$ are symmetric positive semi-definite matrices called the continuous-time and discrete-time state penalty matrices respectively.

4.1 One-dimensional continuous-time system

The first example demonstrates the proposed approach associated with the continuous-time subsystem for a one-state linear system with time variation in the control input function, g, and a quadratic cost. In this example, the analytical solution obtained by solving the differential Riccati equation, as an exact optimal solution, is used to validate the approximate solution:

$$\dot{x} = -x + \sin(t)u_{ct}$$

Using even polynomials in x up to order eight as the basis functions, the stability region and the penalty matrices are chosen as:

$$\boldsymbol{\Phi}_{\mathrm{N}} = \{x^2,\ x^4,\ x^6,\ x^8\} \quad , \quad \Omega = \begin{bmatrix} -1 & 1 \end{bmatrix}$$

$$Q_{ct} = 1 \quad , \quad R_{ct} = 1$$

The numerical results are shown is Figures 2 and 3. As is apparent in Figure 2, the time-varying control gains obtained from the approximation and the Riccati solution are in complete analogy. Interestingly, except for x^2, the control gains associated with the remaining basis elements are all zero consistent with the Riccati solution. This clearly shows that the proposed algorithm associated with the continuous-time subsystem reduces to the differential Riccati equation, and the resulting control law is therefore the exact optimal solution when $V(\boldsymbol{x}, t) := \boldsymbol{x}^{\mathrm{T}}\boldsymbol{P}(t)\boldsymbol{x}$. The time histories of the state and the control effort are also depicted in Figure 3 for $x(0) = 1$.

4.2 Four-dimensional mass-spring system

For this multi-state example, the control of a two-mass two-spring system, shown in Figure 4, is considered. Applying a continuous-time force to mass 1 and a single impulsive action to mass 2, the equations of motion for the system being considered

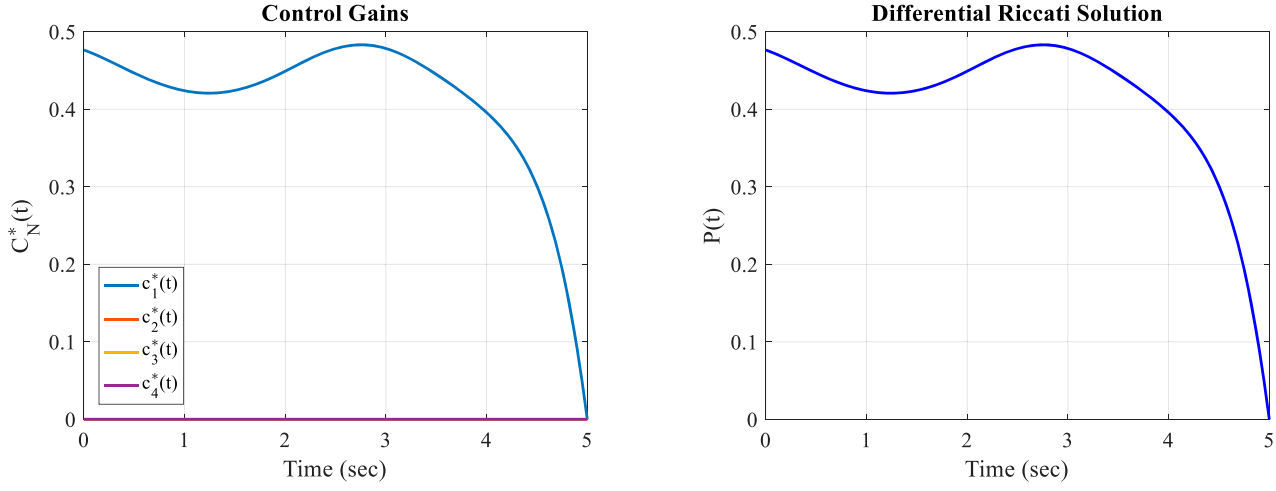

Figure 2. Control gains computed from approximation (left) and Riccati solution (right) for one-dimensional continuous-time linear system.

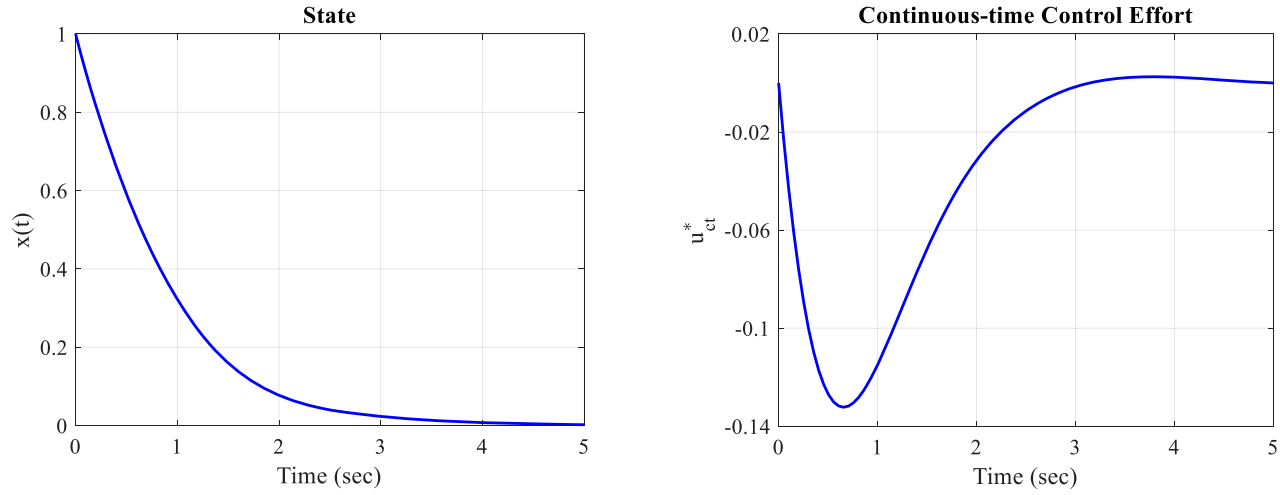

Figure 3. Time histories of the state and the continuous-time control effort for one-dimensional continuous-time linear system.

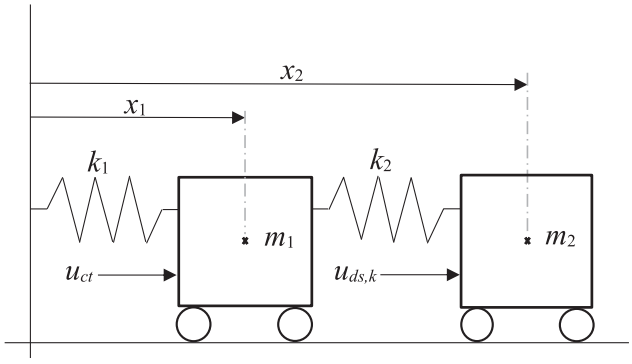

Figure 4. A schematic representation of the two-mass two-spring system.

in a state-space representation can be formulated as:

$$\dot{\boldsymbol{x}} = \begin{bmatrix} x_3 \\ x_4 \\ \frac{k_2x_2+k_2\alpha_2^2x_2^3-k_1x_1-k_1\alpha_1^2x_1^3-k_2x_1-k_2\alpha_2^2x_1^3}{m_1} \\ \frac{k_2x_1+k_2\alpha_2^2x_1^3-k_2x_2-k_2\alpha_2^2x_2^3}{m_2} \end{bmatrix} + \begin{bmatrix} 0 \\ 0 \\ \frac{\cos(\omega t)}{m_1} \\ 0 \end{bmatrix} u_{ct} + \sum_{k=1}^{N_{imp}} \begin{bmatrix} 0 \\ 0 \\ 0 \\ \frac{1}{m_2} \end{bmatrix} u_{ds,k}\delta(t-t_k)$$

where $m_1 = 1\,\text{kg}$, $m_2 = 0.5\,\text{kg}$, $\alpha_1 = 1$, $\alpha_2 = 2$, $k_1 = 1$, $k_2 = 1.5$, $\omega = 1$, and $\delta(t)$ is the Dirac delta function located at each impulse time t_k.

With $\boldsymbol{f}(\boldsymbol{x}, t)$, $\boldsymbol{g}(\boldsymbol{x}, t)$, and $\boldsymbol{B}_{ds}$ coming directly form the equations of motion, the domain of the states and the weighting matrices are determined as follows:

$$\Omega = \begin{bmatrix} -2 & 2 \end{bmatrix}_{x_1} \times \begin{bmatrix} -2 & 2 \end{bmatrix}_{x_2} \times \begin{bmatrix} -1 & 1 \end{bmatrix}_{x_3} \times \begin{bmatrix} -1 & 1 \end{bmatrix}_{x_4}$$

$$\boldsymbol{Q}_{ct} = diag(\ 10^2 \quad 10^2 \quad 10^3 \quad 10^3\ ),\ R_{ct} = 10$$

$$\boldsymbol{Q}_{ds} = diag(\ 10^2 \quad 10^2 \quad 10^3 \quad 10^3\ ),\ R_{ds} = 10^2$$

As is apparent, there are two nonlinear terms in the dynamics of the system, namely x_1^3 and x_2^3. For the control to adequately capture these nonlinear terms, the quadratic basis elements must be thus augmented by some extra higher-order terms. Since x_3 is the only state which corresponds to a non-zero element in $\boldsymbol{g}$, two basis elements in the form of $x_1^3x_3$ and $x_2^3x_3$ are accordingly selected to capture the nonlinear terms involved in the dynamics:

$$\boldsymbol{\Phi}_{\text{N}} = \{x_1^2,\ x_1x_2,\ x_1x_3,\ x_1x_4,\ x_2^2,\ x_2x_3,\ x_2x_4,\ x_3^2,\ x_3x_4,\ x_4^2,\ x_1^3x_3,\ x_2^3x_3\}$$

To find impulsive application times for this example, the so-called guess-and-check approach is employed. In this regard, the hybrid performance index defined by (2) is used as a criterion to determine the time instants which give rise to a minimum performance index.

The time histories of the positions and velocities of m_1 and m_2 for 5 equally spaced impulses with $\boldsymbol{x}(\boldsymbol{0}) = [\,0.1\ -0.2\ 0\ 0\,]^{\text{T}}$ are shown in Figure 5. As is evident, the speed of the response is reasonably quick and well-damped for both position and velocity. In addition, Figure 6 depicts the time histories of the continuous-time and impulsive control inputs for the two-mass two-spring hybrid system wherein both control inputs are stable after 10 s.

5. Conclusion

A novel optimal control design framework for finite-time horizon hybrid nonlinear dynamical systems has been developed in this paper. Assuming a prescribed sequence of impulsive application times, the proposed algorithm simultaneously combined a continuous-time control input with impulsive inputs in an optimal manner. The Galerkin spectral method and the spectral collocation technique were employed to approximate the continuous-time and discrete-time portions of the hybrid Hamilton-Jacobi-Bellman equation respectively. The outcome was therefore a hybrid nonlinear control input which minimised the hybrid performance index being considered. Practical considerations for implementing the proposed hybrid approach were discussed in detail, and the applicability of the algorithm was evaluated through two examples. The proposed hybrid control approach possesses several advantages; 1) the approximate control is in an explicit feedback form with a well-defined

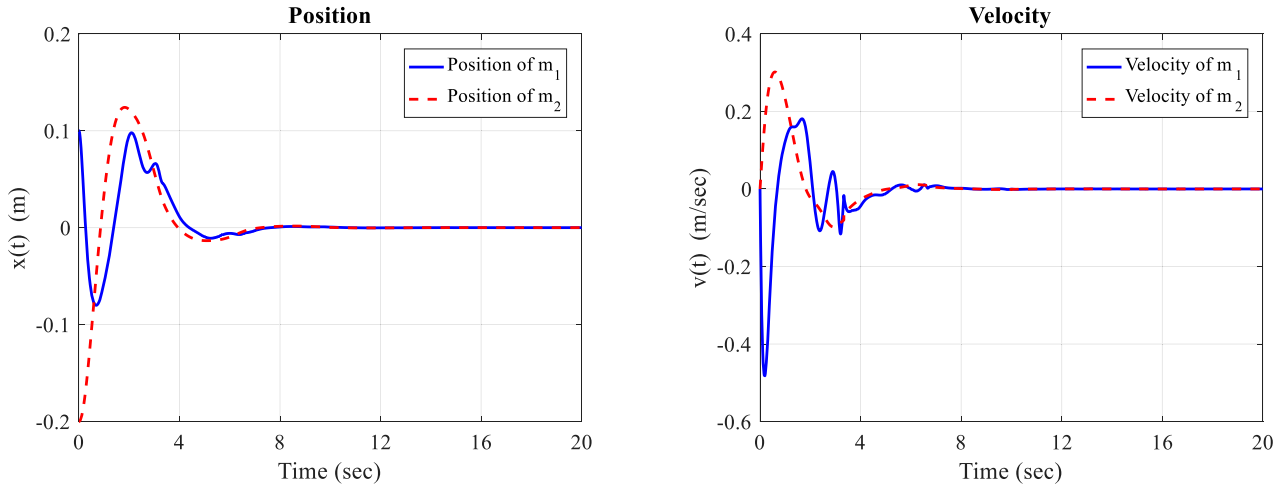

Figure 5. Time histories of the position and velocity for two-mass two-spring hybrid system.

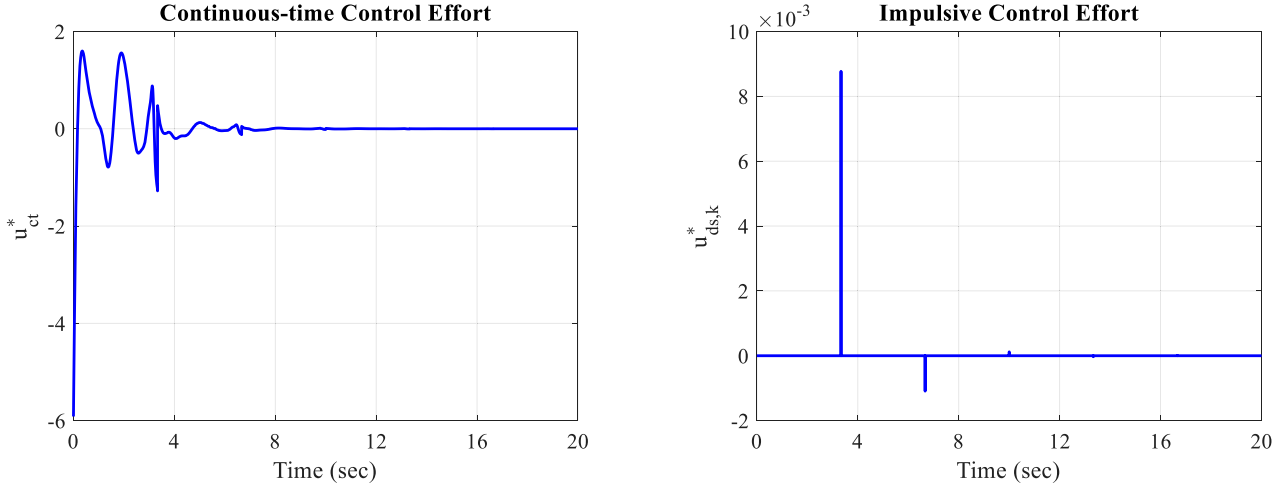

Figure 6. Time histories of the continuous-time and impulsive control inputs for two-mass two-spring hybrid system.

region of stability, 2) as the complexity of the approximation is increased, V_N gradually approaches to V, hence the approximation converges to the optimal control, 3) the control remains stable when the approximation is truncated at a finite degree of complexity, 4) the stability region is specified by the designer, and 5) computations are performed off-line (prior to implementation). On the other hand, the algorithm suffers from the curse of dimensionality as its main drawback. However, there are a variety of possibilities to effectively alleviate the dimensionality problem. The proposed algorithm has been successfully applied to two complex real-world space problems with highly nonlinear nature, namely magnetic/impulsive spacecraft attitude control and Lorentz/impulsive spacecraft formation flying, with significant improvement in the performance of each system. The results on these topics will be the subject of forthcoming papers.

Disclosure statement

No potential conflict of interest was reported by the author(s).

References

Abu-Khalaf, M., & Lewis, F. L. (2005). Nearly optimal control laws for nonlinear systems with saturating actuators using a neural network HJB approach. *Automatica*, *41*(5), 779–791. https://doi.org/10.1016/j.automatica.2004.11.034

Bardi, M., & Capuzzo-Dolcetta, I. (2008). *Optimal control and viscosity solutions of Hamilton–jacobi–bellman equations*. Birkhäuser.

Beard, R. (1995). Improving the Closed-loop Performance of Nonlinear Systems (Doctoral dissertation). Rensselaer Polytechnic Institute, Troy, NY.

Beard, R., & McLain, T. (1998b). Successive Galerkin approximation algorithms for nonlinear optimal and robust control. *International Journal of Control*, *71*(5), 717–743. https://doi.org/10.1080/002071798221542

Beard, R., Saridis, G., & Wen, J. (1996, October). Improving the performance of stabilizing controls for nonlinear systems. *IEEE Control Systems Magazine*, *16*(5), 27–35. https://doi.org/10.1109/37.537206

Beard, R., Saridis, G., & Wen, J. (1997). Galerkin approximations of the generalized Hamilton-Jacobi-Bellman equation. *Automatica*, *33*(12), 2159–2177. https://doi.org/10.1016/S0005-1098(97)00128-3

Beard, R., Saridis, G., & Wen, J. (1998a). Approximate solutions to the time-invariant Hamilton-Jacobi-Bellman equation. *Journal of Optimization Theory and Applications*, *96*(3), 589–626. https://doi.org/10.1023/A:1022664528457

Blaquière, A. (1977). Necessary and sufficient conditions for optimal strategies in impulsive control and applications. In *New trends in dynamic system theory and economics* (pp. 183–213). Academic Press.

Boyce, W. E., & DiPrima, R. C. (1992). *Elementary differential equations and boundary value problems* (pp. 520–531). Wiley.

Bryson, A., & Ho, Y. (1975). *Applied optimal control* (pp. 106–107). Hemisphere Publishing.

Cheng, T., Lewis, F. L., & Abu-Khalaf, M. (2007). A neural network solution for fixed-final time optimal control of nonlinear systems. *Automatica*, *43*(3), 482–490. https://doi.org/10.1016/j.automatica.2006.09.021

Cosmo, M. L., & Lorenzini, E. C. (1997). *Tethers in space handbook* (3rd Ed.). NASA Marshall Spaceflight Center.

Fletcher, C. A. J. (1984). *Computational Galerkin methods*. Springer Series in Computational Physics, Springer-Verlag.

Freeman, R. A., & Kokotovic, P. V. (1995). Optimal nonlinear controllers for feedback linearizable systems. In *Proceedings of the American control Conference* (pp. 2722–2726). https://doi.org/10.1109/acc.1995.532343

Garrard, W. L., & Jordan, J. M. (1977). Design of nonlinear automatic flight control systems. *Automatica*, *13*(5), 497–505. https://doi.org/10.1016/0005-1098(77)90070-X

Haddad, W. M., Chellaboina, V., & Kablar, N. A. (2001). Non-linear impulsive dynamical systems. Part II: Stability of feedback interconnections and optimality. *International Journal of Control*, *74*(17), 1659–1677. https://doi.org/10.1080/00207170110080959

Haddad, W. M., Chellaboina, V., & Nersesov, S. G. (2006). *Impulsive and hybrid dynamical systems*. Princeton University Press.

Hu, J., Wang, H., Liu, X., & Liu, B. (2005). Optimization problems for switched systems with impulsive control. *Journal of Control Theory and Applications*, *3*(1), 93–100. https://doi.org/10.1007/s11768-005-0067-5

Isidori, A. (1989). *Nonlinear control systems* (2nd ed.). Springer.

Lawton, J., & Beard, R. (1998, June). Numerically efficient approximations to the Hamilton-Jacobi-Bellman Equation. Proceedings of the American Control Conference, Philadelphia, PA. IEEE. https://doi.org/10.1109/ACC.1999.786394

Lawton, J., Beard, R., & McLain, T. (1999, June). Successive Galerkin approximation of nonlinear optimal attitude control. In *Proceedings of the American control Conference* (pp. 4373–4377).

Lewis, F. L., Vrabie, D. L., & Syrmos, V. L. (2012). *Optimal control* (3rd ed.). John Wiley & Sons.

Liu, D., Zhang, H., & Wang, F. (2009). Adaptive dynamic programming: An introduction. *IEEE Computational Intelligence Magazine*, *4*(2), 39–47. https://doi.org/10.1109/MCI.2009.932261

Lu, P. (1993). A new nonlinear optimal feedback control law. *Control, Theory and Advanced Technology*, *9*(4), 947–954.

McInnes, C. R. (1999). *Solar sailing: Technology, dynamics and mission applications*. Springer-Praxis.

McLain, T., & Beard, R. (1997). Nonlinear optimal control of a hydraulically actuated positioning system. In *Proceedings of the ASME international mechanical engineering congress and exposition, fluid power systems and technology division* (pp. 163–168).

McLain, T., & Beard, R. (1998a). Nonlinear optimal control of an underwater robotic vehicle. International conference on robotics and automation. Leuven, Belgium.

McLain, T., & Beard, R. (1998b). Nonlinear optimal control design of a missile autopilot. AIAA Guidance, Navigation and Control Conference, Boston, MA.

Nijmeijer, H., & van der Schaft, A. J. (1990). *Nonlinear dynamical control systems*. Springer.

Nishikawa, Y., Sannomiya, N., & Itakura, H. (1971). A method for suboptimal design of nonlinear feedback systems. *Automatica*, *7*(6), 703–712. https://doi.org/10.1016/0005-1098(71)90008-2

Quarteroni, A., Sacco, R., & Saleri, F. (2000). *Numerical mathematics*. Springer-Verlag.

Richardson, S., & Wang, S. (2006). Numerical solution of Hamilton-Jacobi-Bellman equations by an exponentially fitted finite volume method. *Optimization*, *55*(1–2), 121–140. https://doi.org/10.1080/02331930500530237

Sharifi, E., & Damaren, C. J. (2019). Nonlinear optimal approach to spacecraft formation flying using lorentz force and impulsive thrusting, manuscript submitted for publication.

Sharifi, E., & Damaren, C. J. (2020a). Nonlinear optimal approach to magnetic spacecraft attitude control, AIAA Guidance, Navigation, and Control Conference, Orlando, FL.

Sharifi, E., & Damaren, C. J. (2020b). Nonlinear optimal approach to spacecraft attitude control using magnetic and impulsive actuations. *Journal of Guidance, Control and Dynamics*, accepted for publication. https://doi.org/10.2514/1.G004913

Sobiesiak, L. A., & Damaren, C. J. (2015a). Optimal continuous/impulsive control for Lorentz-augmented spacecraft formations. *Journal of Guidance, Control and Dynamics*, *38*(1), 151–157. https://doi.org/10.2514/1.G000334

Sobiesiak, L. A., & Damaren, C. J. (2015b). Impulsive spacecraft formation Manoeuvres with optimal firing times. *Journal of Guidance, Control, and Dynamics*, *38*(10), 1994–1999. https://doi.org/10.2514/1.G001095

Sobiesiak, L. A., & Damaren, C. J. (2016). Lorentz-augmented spacecraft formation reconfiguration. *IEEE Transactions on Control Systems Technology*, *24*(2), 514–524. https://doi.org/10.1109/TCST.2015.2461593

Wang, S., Jennings, L. S., & Teo, K. L. (2003). Numerical solution of Hamilton–jacobi–bellman equations by an upwind finite volume method. *Journal of Global Optimization*, *27*(2), 177–192. https://doi.org/10.1023/A:1024980623095